



**HAL**  
open science

## How old is the Baikal Rift Zone? Insight from apatite fission track thermochronology

Marc Jolivet, Thomas de Boisgrollier, Carole Petit, Marc Fournier, V. A. Sankov, Jean-Claude Ringenbach, L. Byzov, A. I. Miroshnichenko, Sergei N. Kovalenko, S. V. Anisimova

### ► To cite this version:

Marc Jolivet, Thomas de Boisgrollier, Carole Petit, Marc Fournier, V. A. Sankov, et al.. How old is the Baikal Rift Zone? Insight from apatite fission track thermochronology. *Tectonics*, 2009, 28, pp.TC3008. 10.1029/2008TC002404 . hal-00420895

**HAL Id: hal-00420895**

**<https://hal.science/hal-00420895>**

Submitted on 30 Apr 2021

**HAL** is a multi-disciplinary open access archive for the deposit and dissemination of scientific research documents, whether they are published or not. The documents may come from teaching and research institutions in France or abroad, or from public or private research centers.

L'archive ouverte pluridisciplinaire **HAL**, est destinée au dépôt et à la diffusion de documents scientifiques de niveau recherche, publiés ou non, émanant des établissements d'enseignement et de recherche français ou étrangers, des laboratoires publics ou privés.

## How old is the Baikal Rift Zone? Insight from apatite fission track thermochronology

M. Jolivet,<sup>1</sup> T. De Boisgrollier,<sup>2</sup> C. Petit,<sup>2</sup> M. Fournier,<sup>2</sup> V. A. Sankov,<sup>3</sup> J.-C. Ringenbach,<sup>4</sup> L. Byzov,<sup>3</sup> A. I. Miroshnichenko,<sup>3</sup> S. N. Kovalenko,<sup>3</sup> and S. V. Anisimova<sup>3</sup>

Received 8 October 2008; revised 2 March 2009; accepted 10 April 2009; published 20 June 2009.

[1] Apatite fission track analysis (AFTA) data are used to bring new light on the long-term and recent history of the Baikal rift region (Siberia). We describe the evolution of the topography along a NW–SE profile from the Siberian platform to the Barguzin range across the Baikal–southern Patom range and the northern termination of Lake Baikal. Our results show that the Baikal–Patom range started to form in the Early Carboniferous and was reactivated in Middle Jurassic–Lower Cretaceous times during the orogenic collapse of the Mongol–Okhotsk belt. Samples located in the Siberian platform recorded a continuous sedimentation up to the early Carboniferous but remain unaffected by later tectonic episodes. The Barguzin basin probably started to form as early as Late Cretaceous, suggesting a continuum of deformation between the postorogenic collapse and the opening of the Baikal Rift System (BRS). The initial driving mechanism for the opening of the BRS is thus independent from the India–Asia collision. AFTA show a late Miocene–early Pliocene increase in tectonic extension in the BRS that confirms previous thoughts and might reflect the first significant effect of the stress field generated by the India–Asia collision.

**Citation:** Jolivet, M., T. De Boisgrollier, C. Petit, M. Fournier, V. A. Sankov, J.-C. Ringenbach, L. Byzov, A. I. Miroshnichenko, S. N. Kovalenko, and S. V. Anisimova (2009), How old is the Baikal Rift Zone? Insight from apatite fission track thermochronology, *Tectonics*, 28, TC3008, doi:10.1029/2008TC002404.

### 1. Introduction

[2] The Baikal Rift System (BRS) (Figures 1 and 2) is a key feature of the tectonic evolution of Asia but, despite a large number of geological and geophysical studies, its age and origin are still largely debated. Two main hypotheses are proposed [Sengör and Burke, 1978]: (1) the “active rift

hypothesis” considers that rifting is induced by the effects of a wide asthenospheric diapir acting on the base of the crust beneath the rift axis [e.g., Logatchev and Zorin, 1987; Windley and Allen, 1993; Gao et al., 2003; Kulakov, 2008] and (2) for the “passive rift hypothesis” the BRS is a kind of pull-apart basin opening in response to the India–Asia collision to the south [e.g., Molnar and Tapponnier, 1975; Tapponnier and Molnar, 1979; Zonenshain and Savostin, 1981; Cobbold and Davy, 1988; Petit et al., 1996; Lesne et al., 1998; Petit and Déverchère, 2006].

[3] Recent geophysical investigations tend to demonstrate that there is no hot mantle plume beneath the Baikal rift [e.g., Ivanov, 2004; Tiberi et al., 2003; Lebedev et al., 2006; Petit et al., 2008]. Furthermore, mantle plume activity is most certainly not sufficient to produce rifting without a prerift favorable structural inheritance [Zorin et al., 2003]. Problems also arise in the “passive rift hypothesis” because the indentation of Asia by India mostly generated compressive structures such as the Tibet plateau, the central Asian ranges or large transpressive lithospheric faults like in Mongolia. Only the occurrence of favorably oriented inherited structures along the eastern margin of the Siberian craton can explain the development of extensional structures in this general compressive context.

[4] From the Eocene to the middle Miocene, distributed extension prevailed in Asia within a wide region extending from the Baikal rift to the Okhotsk Sea and to SE Asia and Indonesia. On the eastern and southeastern margins of Asia, major marginal basins opened above the western Pacific subduction zones, and in interior Asia a number of continental rifts developed in northern China and the Baikal rift region. Several studies explored the far-field effects of the India–Asia collision in northeast Asia interacting with subduction-related extension [Kimura and Tamaki, 1986; Davy and Cobbold, 1988; Jolivet et al., 1990, 1992; Delvaux, 1997; Worrall et al., 1996; Fournier et al., 1994, 2004].

[5] Within all these different models, the chronology of reactivation of the inherited structures is a first-order parameter needed to constrain the geodynamic evolution of central Asia. The chronology of the Baikal rift evolution is based on sedimentology data acquired in the various basins forming the rift system, but the onset of formation and the evolution of the topography surrounding the BRS (in the Khamar Daban and Patom ranges for example) have poorly been explored up to now. In the north Baikal rift, this topography does not have a gravity signature compatible with rift shoulders [Petit et al., 2002] and may thus not be directly related to rifting.

<sup>1</sup>Laboratoire Géosciences Montpellier, UMII, UMR 5243, Université Montpellier II, CNRS, Montpellier, France.

<sup>2</sup>Laboratoire de Tectonique, UMR 7072, Université Pierre et Marie Curie–Paris 6, CNRS, Paris, France.

<sup>3</sup>Institute of the Earth Crust, Irkutsk, Russia.

<sup>4</sup>Total, Courbevoie, France.

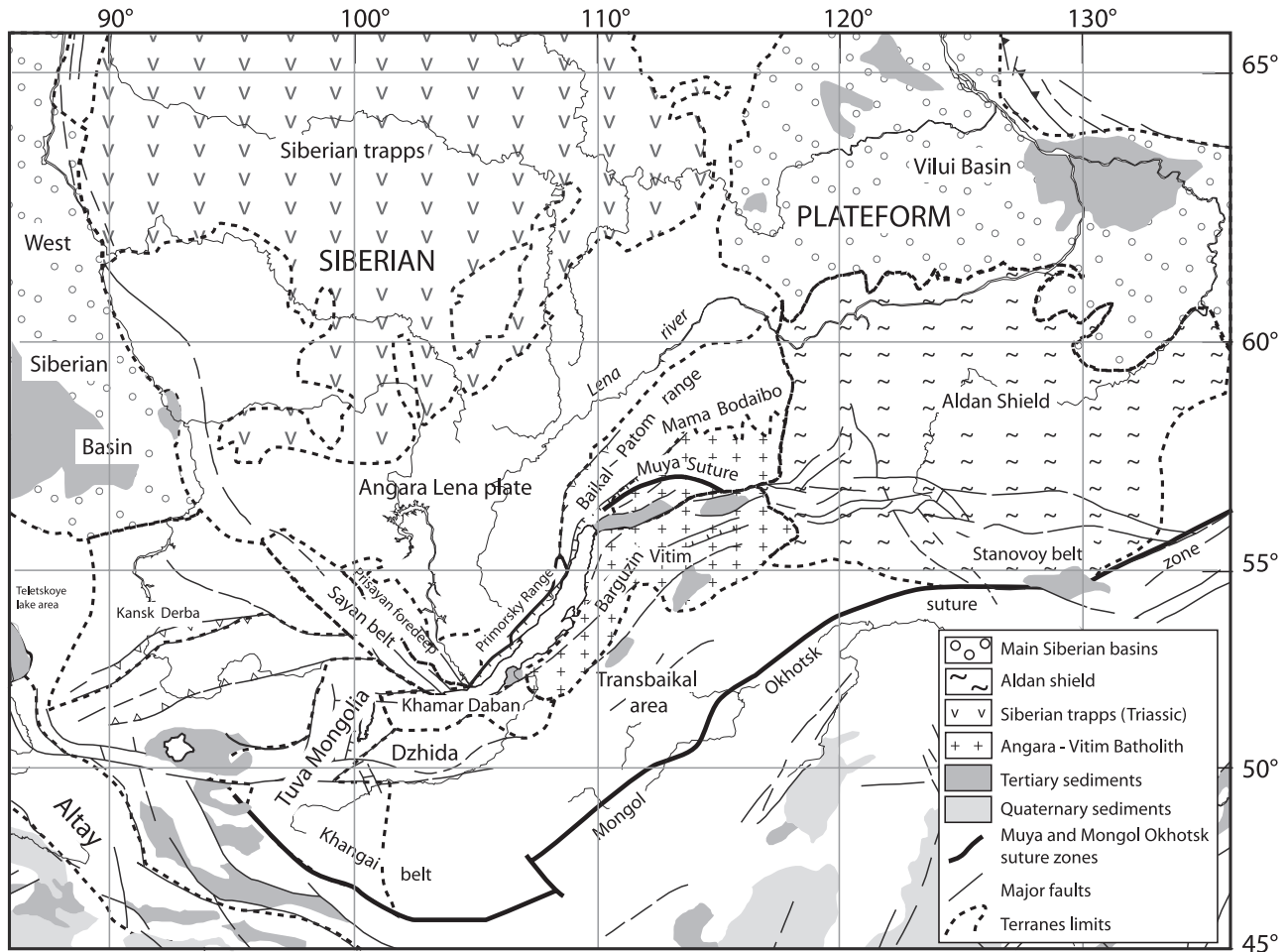


**Figure 1.** Simplified map of the various terranes and structures of eastern Siberia and northern Mongolia. The major tertiary and quaternary basins are also indicated. Position of the structures and terranes were determined using maps from *Delvaux et al.* [1995a, 1997], *Gusev and Khain* [1996], and *Malitch* [1999].

[6] The modality of development of the rift itself is also debated. The most frequently admitted idea describes an initial “slow rifting” stage lasting from late Oligocene to late Pliocene followed by a “fast rifting” stage from late Pliocene to Present [e.g., *Logatchev and Zorin*, 1987; *Logatchev*, 1993, 2003; *Mats*, 1985, 1993; *Mats et al.*, 2001; *Petit and Déverchère*, 2006]. However, this two-stage development has been questioned by *ten Brink and Taylor* [2002] on the basis of a deep seismic refraction profile across Lake Baikal.

[7] A first apatite fission track study by *van der Beek et al.* [1996] highlights the importance of an Early Cretaceous denudation event south of Lake Baikal, in the Primorsky range, the Olkhon area and the Khamar Daban Mountains. However, these authors do not provide information on the older and younger events that possibly affected the region.

[8] In this work, we present new apatite fission track thermochronologic results that help us constrain the time of formation and the evolution of the relief around the northern part of Lake Baikal in the Baikal–southern Patom range and

in the Barguzin range. We reconstruct the thermal history of samples collected along a broadly W–E transect running from the Siberian platform to the Barguzin basin across the Baikal–southern Patom ranges and the Baikal rift.

[9] The new data presented in this work describe the successive episodes of relief building, sedimentation and erosion that occurred from the Early Ordovician to Present in the different tectonic units of the transect. They bring new information on the timing, amount and possibly the mechanisms of relief building around the present-day Baikal and Barguzin basins.

## 2. Geology and Tectonic Setting of the Baikal Rift System

### 2.1. Archean and Proterozoic History

[10] The basement of the Siberian platform (Figure 1) is made of Archean continental crust [e.g., *Khain and Bozhko*, 1988; *Dobretsov et al.*, 1992; *Delvaux et al.*, 1995a; *Gusev and Khain*, 1996]. Around 1900–1700 Ma the Siberian

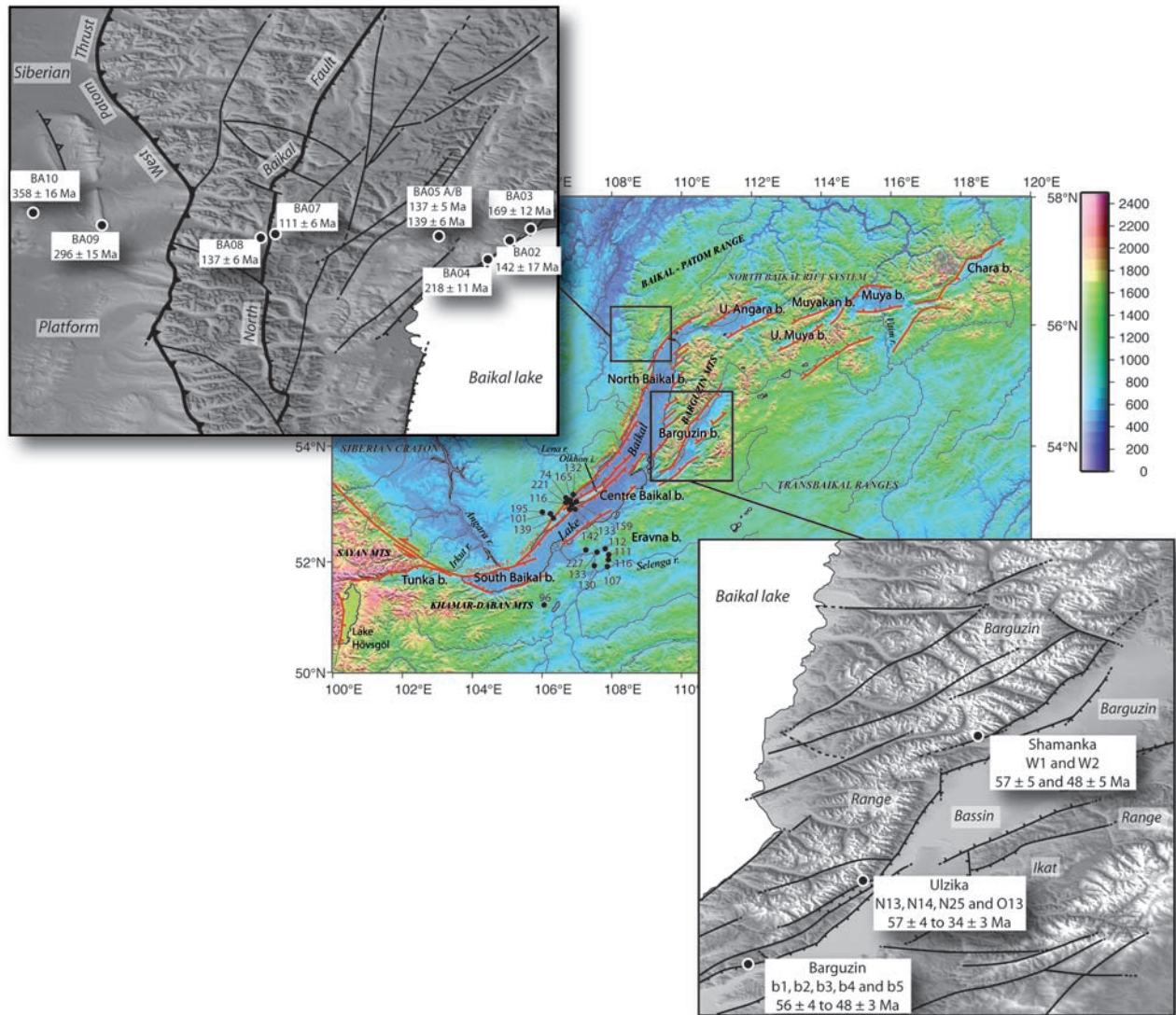


**Figure 2.** General topography, geography, and fault pattern of the Baikal area with details of the areas sampled in this work. Samples numbers and ages from our study are indicated. Ages from *van der Beek et al.* [1996] are also noted.

craton grows by the accretion of Archean blocks, which induces compressional deformation, plutonism, and metamorphism [e.g., *Gusev and Khain, 1996*]. During the Riphean, rifting occurs in several places leading to the formation of intracontinental basins and of a passive margin along the southern border of the craton, north of the Paleo-Asian ocean [*Zonenshain et al., 1990a, 1990b; Dobretsov et al., 1992; Belichenko et al., 1994; Delvaux et al., 1995a; Gusev and Khain, 1996*]. Several microcontinents are scattered in this ocean: the Khamar Daban, Barguzin, Tuva-Mongolia, and Kansk-Derba blocks (Figure 1) [*Belichenko et al., 1994; Berzin et al., 1994; Melnikov et al., 1994; Delvaux et al., 1995a*]. In the late Riphean, a thick series of flysch deposited in the Bodaibo region marks the onset of passive margin inversion. However, this deformation does not appear to affect the area extending southward

from the Patom zone to the Siberian platform [*Gusev and Khain, 1996*]. Docking against the craton of the various terranes wandering in the Paleo-Asian ocean starts in the Vendian [*Delvaux et al., 1995a*] and causes the formation of large foredeeps along the southern margin of the Siberian platform, which accumulate sediments until the Early Silurian [*Melnikov et al., 1994*].

## 2.2. Vendian and Paleozoic History

[11] Thick Vendian molasses deposits in the Mama-Bodaibo area (Figure 1), as well as a 600–550 Ma metamorphic and plutonic event recorded in the Baikal-Muya ophiolite belt indicate that the Barguzin block collides with the Siberian platform in Vendian–Early Cambrian times [e.g., *Berzin and Dobretsov, 1994; Delvaux*

*et al.*, 1995a; *Gusev and Khain*, 1996]. In the Late Cambrian–Early Ordovician, the Tuva–Mongolia microcontinent collides with the Angara–Lena plate (Figure 1) on the southern margin of the Siberian platform, separating the Paleo-Asian ocean in two branches: the paleo-Mongol–Okhotsk to the east and the western Paleo-Asian ocean to the west [*Zorin et al.*, 1993; *Delvaux et al.*, 1995a]. This episode coincides with a stage of regional metamorphism dated around 530–485 Ma along the eastern margin of the platform [*Bibikova et al.*, 1990; *Sryvtsev et al.*, 1992; *Bukharov et al.*, 1992; *Fedorovskii et al.*, 1993]. A Late Silurian–Early Devonian deformation phase possibly related to the collision between the Dzhida island arc and the Tuva–Mongolia and Khamar Daban–Barguzin blocks affects the area between the southeast margin of the Siberian platform and the Khamar Daban–Barguzin block [*Gibsher et al.*, 1993; *Delvaux et al.*, 1995a]. After this episode, a new subduction zone develops behind the accreted terranes, followed by a massive granite emplacement (the Angara–Vitim batholith) (Figure 1) in the Dzhida, Khamar Daban–Barguzin and Stanovoy regions. Granites yielded U–Pb and Rb–Sr ages ranging from 285 to 339 Ma [*Yarmolyuk et al.*, 1997]. This magmatic episode marks the final closure of the Paleo-Asian ocean [*Delvaux et al.*, 1995a]. By Late Carboniferous a subduction-accretion wedge develops south of the Dzhida, Khamar Daban–Barguzin and Stanovoy terranes, which is afterward dismembered along strike by later tectonic movements [*Zorin*, 1999].

[12] The main tectonic structures of the Baikal–Patom and Zhuya fold-and-thrust belts seem to develop at the end of this episode of subduction and collision. However, except some small outcrops of Devonian sediments along the remote northern edge of the Patom belt, no sediments derived from the erosion of these reliefs have remained preserved. Consequently the tectonics of the Baikal–Patom belt is not precisely dated.

[13] The lack of post-Silurian sediments makes it very difficult to describe the evolution of the Siberian platform during middle-late Paleozoic. However, except on its margins, the Siberian craton remained stable during most of the Paleozoic and the outcropping Ordovician and Silurian series are only weakly deformed [e.g., *Gusev and Khain*, 1996; *Cocks and Torsvik*, 2007].

[14] West of the Khamar Daban area, western Mongolia collides with Siberia in the Early Permian [*Zonenshain et al.*, 1990a; *Nie et al.*, 1990] which marks the beginning of closure of the Mongol–Okhotsk ocean (Figure 1). By early Late Permian–Early Triassic, north China collides with Mongolia forming the Mongolia–north China continent [*Zonenshain et al.*, 1990a; *Zhao et al.*, 1990; *Enkin et al.*, 1992; *Zorin et al.*, 1993, 1994; *Zorin*, 1999; *Lin et al.*, 2008].

### 2.3. Mesozoic History

[15] In the Khangai zone, granitoid magmatic activity continues from Late Permian to Early Jurassic times [*Filippova*, 1969] indicating continuous subduction of the Mongolia–north China margin under Siberia and thickening of the crust [*Zorin et al.*, 1990].

[16] In the early Middle Jurassic, marine sedimentation in the Trans-Baikal region is replaced by syntectonic conglomerates, gravels and sandstones of continental origin [*Mushnikov et al.*, 1966; *Ermikov*, 1994]. This seems to indicate the final closure of the Mongol–Okhotsk ocean and the development of the Mongol–Okhotsk orogen. However, using paleomagnetic data, *Enkin et al.* [1992] and *Metelkin et al.* [2007] calculated that by late Middle–early Late Jurassic, the Mongol–Okhotsk ocean was not completely closed and might still be up to 1000 km wide. The oceanic basin was closing from west to east due to a clockwise rotation of the Siberian block relative to Mongolia [e.g., *Kazansky et al.*, 2005; *Metelkin et al.*, 2004, 2007]. Rotation of Siberia induced large strike-slip motion that induced extension in the Trans-Baikal area [e.g., *Delvaux*, 1997; *Metelkin et al.*, 2007]. Only by the Early Cretaceous, the concordance between the paleomagnetic poles of Siberia, Europe and Southeastern Asia indicates the complete closure of the Mongol–Okhotsk ocean [*Kravchinsky et al.*, 2002; *Metelkin et al.*, 2004, 2007] and the continental collision.

[17] The compressive deformation associated to the closure of the Mongol–Okhotsk ocean is recorded in the whole Sayan–Baikal belt (Figure 1) [*Ermikov*, 1994; *Delvaux et al.*, 1995a, *Delvaux*, 1997]. On the southern and eastern margins of the Siberian platform, the Sayan–Angara and Stanovoy foredeep basins develop and Early–Middle Jurassic continental molasses accumulate (Figure 1).

[18] Apatite fission track data obtained from the southern end of Lake Baikal suggest that synorogenic exhumation takes place during the Early Cretaceous in that area [*van der Beek et al.*, 1996]. Farther to the west, in the lake Teletskoye region (northern Altay) (Figure 1), apatite fission track data [*De Grave and Van den haute*, 2002] record a Early Cretaceous cooling event that induced up to 1500–2000 m of denudation. As for the Late Carboniferous topography of the Patom range, there is no indication of Jurassic or Cretaceous sediments preserved along the western margin of the Baikal range. This is largely inconsistent with the existence of a tectonic relief in that area, but also with the evidences of denudation reported by *van der Beek et al.* [1996]. One possibility would be that the sediments produced by erosion of the Patom and Baikal ranges have been transported by a river system similar to the present-day Lena river system (i.e., the Lena river drainage system including numerous tributaries draining the Patom and Baikal ranges), to the Vilui basin and the Arctic ocean (Figure 1) where Jurassic and Cretaceous detrital deposits are found [e.g., *Prokopiev et al.*, 2008; *Spicer et al.*, 2008].

[19] In late Late Jurassic and Early Cretaceous, prior to or possibly contemporaneously to the final collision along the eastern termination of the Mongol–Okhotsk suture zone, intensive extensional deformation leading to the formation of basins and metamorphic core complexes affects a huge area encompassing the southern margin of the Baikal–Vitim terrane, the Transbaikalian area of the Mongol–Okhotsk belt, southern Mongolia and northern China [e.g., *Zheng et al.*, 1991; *van der Beek et al.*, 1996; *Davis et al.*, 1996,

2001, 2002; *Webb et al.*, 1999; *Zorin*, 1999; *Darby et al.*, 2001b; *Meng*, 2003; *Fan et al.*, 2003; *Wang et al.*, 2006]. This extension is associated with intensive magmatism and plutonism [e.g., *Tauson et al.*, 1984; *Rutshtein*, 1992; *Gusev and Khain*, 1996; *Chen and Chen*, 1997; *Graham et al.*, 2001]. The chemical and isotopic composition of these magmas indicates a mixture between a crustal and a mantle source [*Tauson et al.*, 1984; *Shao et al.*, 2001; *Yarmolyuk and Kovalenko*, 2001; *Fan et al.*, 2003]. Collision between Siberia and the Mongolia–north China block leads to a strong compressive deformation recorded in Mongolia and north China [e.g., *Zheng et al.*, 1996, 1998; *Song and Dou*, 1997; *Chen*, 1998; *Jin et al.*, 2000; *Darby et al.*, 2001a; *Yang et al.*, 2001; *Lin et al.*, 2008]. The Mongolian crust is then strongly thickened, reaching up to 60 km in the Khangai belt of central Mongolia [e.g., *Zorin*, 1999; *Zorin et al.*, 1993, 2002; *Suvorov et al.*, 2002]. This overthickening of the crust probably causes large body forces responsible for postorogenic collapse [*Graham et al.*, 2001; *Fan et al.*, 2003].

[20] However, the mechanism responsible for the late Late Jurassic–Cretaceous extension is still debated and several alternative models have been proposed: back-arc extension caused by rollback of the subducting paleo-Pacific plate [*Watson et al.*, 1987; *Traynor and Sladen*, 1995], magmatic underplating [*Shao et al.*, 2000; *Ren et al.*, 2002], gravitational collapse of the overthickened crust [*Graham et al.*, 2001; *Fan et al.*, 2003], transtensional faulting related to extrusion tectonics [*Kimura et al.*, 1990; *Ren et al.*, 2002], break-off of the northward subducted Mongol–Okhotsk oceanic slab [*Meng*, 2003], shear delamination of the lithosphere and mantle upwelling [*Wang et al.*, 2006].

#### 2.4. Cenozoic History

[21] During Late Cretaceous–Paleogene, a planation surface develops in the southeastern Baikal and western Transbaikalian regions, covered by a lateritic-kaolinic weathering crust [*Mats*, 1993; *Kashik and Masilov*, 1994; *Logatchev et al.*, 2002]. Meanwhile, the extension that was active during the Mesozoic is still going on. The formation of the South Baikal Depression in Late Cretaceous–early Paleogene [*Logatchev et al.*, 1996; *Logatchev*, 2003] is considered by *Tsekhovskiy and Leonov* [2007] as the onset of extensional tectonics in the future Baikal rift. Other smaller depressions sometimes associated with weak volcanism start to develop in the western Transbaikalian region [e.g., *Bazarov*, 1986; *Logatchev et al.*, 1996; *Yarmolyuk and Ivanov*, 2000; *Mats et al.*, 2001]. Late Cretaceous–Eocene sediments are found in the north Baikal and Tunka basin [*Mats*, 1993; *Scholz and Hutchinson*, 2000], but are probably derived from in situ erosion rather than real rift sedimentation [*Kashik and Masilov*, 1994].

[22] In the late Oligocene–Miocene, rifting of the BRS starts in the Tunka, north Baikal and central Baikal basins [e.g., *Mats*, 1993, 1985; *Mats et al.*, 2001; *Logatchev*, 1993, 2003]. From late Oligocene to early Pliocene, the “slow rifting” phase is characterized by the dismembering of the

planation surface by tectonic extension, leading to the formation of numerous grabens in Baikal and Transbaikalian region. Within the Baikal area, this initial phase is characterized by fine grained sandstones, coal-bearing molasses, lacustrine clays and siltstones typical of a slowly subsiding wide lakes environment [e.g., *Nikohyev et al.*, 1985; *Moore et al.*, 1997; *Levi et al.*, 1997; *Mats et al.*, 2000]. These sediments are sometimes folded and faulted, especially within Lake Baikal [e.g., *Levi et al.*, 1997]. Simultaneously, thick alkaline and subalkaline basalt sequences (mostly Miocene in age) are emplaced in the Udokan, Vitim and Khमार Daban region [*Kiselev et al.*, 1978; *Bazarov*, 1986; *S. V. Rasskasov et al.*, Late Cenozoic volcanism in the Baikal Rift System: Evidence for formation of the Baikal and Khubsugul basins due to thermal impacts on the lithosphere and collision-derived tectonic stress, paper presented at SIAL III: The Third International Symposium on Speciation in Ancient Lakes, Russian Academy of Sciences, Irkutsk, Russia, 2–7 September 2002]. Chemical and isotopic data obtained from Mongolian basalts indicate that these lavas formed at a depth of at least 70 km from recently metasomatised lithosphere [*Barry et al.*, 2003].

[23] The “fast rifting” phase, which is still going on, starts in the late Pliocene with the rapid development of the whole Baikal rift (deepening and extension), and the onset of relief building in the Baikal and Transbaikalian region [e.g., *Hutchinson et al.*, 1992; *Delvaux et al.*, 1995b, 1997]. The transition between the first and second phase is marked by middle to upper Pliocene coarse-grained sandstones and conglomerates (the Anosov formation onshore) unconformably overlying the Miocene formations [*Nikohyev et al.*, 1985]. These sediments are recognized in nearly all basins of the rift system suggesting that the present-day geometry was acquired at that time [*Petit and Déverchère*, 2006]. However, *Mats et al.* [2000] suggested that the transition between “slow rifting” and “fast rifting” is diachronous, starting in upper Miocene (10–7 Ma) in the deepest areas and progressively onlapping on the relief up to 4 Ma. The “fast rifting” phase corresponds, in the deep north Baikal basin to a thick series of turbidites [*Kuzmin et al.*, 2000] appearing as parallel, continuous reflectors onlapping on the older, coarser units with an angular and/or erosional unconformity [e.g., *Moore et al.*, 1997]. Using paleomagnetic data, *Kuzmin et al.* [2000] dated the unconformity around 2.5 Ma.

[24] On the basis of fault slickenslide measurements in recent sediments, *Delvaux et al.* [1997] proposed that from Oligocene to middle Miocene, a transpressive strike slip regime prevailed with a maximum horizontal stress oriented NW–SE in the Tunka basin and NE–SW in the Barguzin and central Baikal basins. The regional stress regime switches to transtension or pure extension during upper Miocene probably due to a general kinematic reorganization of the Baikal rift system. *Vassallo et al.* [2007] and *Jolivet et al.* [2007] showed using fission track data that the Cenozoic uplift of the Gobi Altay initiated around  $5 \pm 3$  Ma due to the propagation of the compressive deformation from the south. Similar evidences of increase in cooling rates are reported

by *De Grave and Van den haute* [2002] from the lake Teletskoye area of northern Altay and by *Delvaux et al.* [1995b] in the Kurai-Chuya depression again in Altay. Finally, *Larroque et al.* [2001] reported evidences of Pleistocene-Holocene inversion of the north Tunka normal fault, implying a continuing increase of the north–northeastward compressive stress.

[25] It is again important to note that if Cenozoic topography indubitably developed along the western margin of the Baikal rift, there are still only few evidences on the Siberian craton of Tertiary sediments that could derive from its erosion. Only Quaternary detrital deposits are mapped along that relief (if we do not take into account the small, thin outcrops of Neogene lacustrine sediments). Even if the initial sedimentation rates were very slow and sedimentation was very diffuse, some of these deposits should have been preserved. Nowadays, the large Lena and Vitim river systems efficiently carry the sediments northward up to the Vilui basin and the Arctic Ocean, whereas only a small amount of the relief area is drained toward the various basins of the BRS.

### 3. Apatite Fission Track Analysis

#### 3.1. Sampling and Methodology

[26] We collected samples west of Lake Baikal along an E–W section running from the Siberian platform to the lake's shore across the Baikal range (Figure 2). East of the lake, samples were collected along three topographic profiles in the Barguzin range: the Shamanka profile to the north, the Ulzika profile in the central part of the Barguzin range and the Barguzin profile to the south (Figure 2). The altitude and position of the samples were monitored using a portable GPS and Russian topographic maps. Samples are essentially granites and gneisses except for samples BA09 and BA10 which are Early Ordovician red sandstones (Table 1). Apatite samples were prepared for AFT analysis following the standard method [*Hurford*, 1990]. Mean fission track ages were obtained using the zeta calibration method [*Hurford and Green*, 1983] with a zeta value of  $358.96 \pm 4.35$  (T. Boisgrollier) or  $342.04 \pm 19.7$  (M. Jolivet), obtained on both Durango and Mont Dromedary apatite standards. Spontaneous fission tracks were etched using 6.5% HNO<sub>3</sub> for 45 s at 20°C. Induced fission tracks were etched using 40% HF for 40 min at 20°C. Samples were irradiated at the OSU facility, Oregon. Fission tracks were counted and measured on a Zeiss Axioplan 2 microscope, using a magnification of 1250 under dry objectives. All ages that will be discussed below are central ages. The results are given in Table 1 together with a complete description of the analytical procedure.

#### 3.2. Results

[27] The fission track ages can be divided in three groups corresponding to three morphological zones (Figure 2):

[28] 1. On the Siberian platform, the samples have Devonian and Carboniferous ages.

[29] 2. In the Baikal range, all samples except BA04 have middle Jurassic to lower Cretaceous ages. Sample BA04 is

slightly older (upper Triassic) but the ages of the individual grains appear to be split in two populations which explains the  $P(\chi^2)$  value close to 0. This may be due to variable chemical compositions of the apatite crystals [e.g., *O'Sullivan and Parrish*, 1995; *Barbarand et al.*, 2003]. However, the younger age population in this sample gives a mean value around 180 Ma, which is consistent with the ages of the surrounding samples (Figure 3). The older age population gives a mean value of circa 350 Ma, similar to the age of the Siberian platform. Besides different AFT ages, the Siberian platform and the Baikal range are two different tectonic units marked by a sharp step in the topography (Figure 2). Sample BA07 in the center of the Baikal range is younger suggesting either internal differential movements, or stronger or later erosion in the center of the range.

[30] 3. In the Barguzin range, ages are divided in two groups depending on the altitude. The highest samples, between ~2150 m (samples W1) and ~1300 m (sample b5) provided Paleocene to early Eocene ages. The samples N25 and O13 which were collected at 900 m and 800 m respectively provided early Oligocene (Rupelian) ages. There is no indication of Mesozoic ages in this area. Sample N14 has a slightly older age compared to the others and especially to sample N13 located at a higher altitude and thus potentially older. This, like for sample BA04 may be due to differences in chemical composition.

[31] The three cooling periods are also well illustrated on the age versus altitude and mean fission track lengths plots of all the samples along the section (Figures 4a and 4b) with a first cooling episode during the late Jurassic–early Cretaceous; a second, stronger cooling event in early Paleocene and finally a third, less documented cooling in early Oligocene. When plotted on a similar graph, the data obtained by *van der Beek et al.* [1996] confirm the late Jurassic–early Cretaceous episode (Figures 4c and 4d) which thus appears generalized around the Baikal lake. On the age versus altitude plot (Figure 4d), data from the Primorski area provide a link between the Mesozoic and Cenozoic denudation events.

[32] The apatite fission track age integrates the whole thermal history of the rocks between ~110°C and 60°C. In order to better constrain the cooling history of the three main zones described above, reverse modeling of track lengths distribution has been performed using the AFTSolve software [*Ketcham et al.*, 2000] and the *Laslett et al.* [1987] annealing model. These models are only valid within the fission track partial annealing zone (PAZ), between 60 and 110°C.

#### 3.3. Low-Temperature Evolution of the Siberian Platform

[33] Samples BA10 and BA09 (Figure 5a) experienced a period of heating from early Ordovician (the estimated sedimentation age) up to late Devonian. This heating, due to burying by continuous sedimentation is higher for sample BA09, which is most probably completely reset. Sample BA09 crosses the 110°C isotherm between 350 and 320 Ma (early Carboniferous). Between 320 and 300 Ma the cooling

**Table 1.** Apatite Fission Track Analysis Data<sup>a</sup>

Sample	Rock Type	Lat/Long	Alt	Nb	$\rho_d \times 10^4$	$\rho_s \times 10^4$	$\rho_t \times 10^4$	[U]	$P(\chi^2)$	Var	MTL ( $\pm 1\sigma$ )	FT Age ( $\pm 2\sigma$ )
BA09	Ordovician red sandstone	N55°46'26.7"/E108°15'35.8"	934	15	114.2 (10714)	344.3 (1033)	233.3 (700)	25	80	5.9	13.0 $\pm$ 0.2 (100)	295.6 $\pm$ 15.2
BA10	Ordovician red sandstone	N55°49'51.8"/E108°04'54.0"	513	20	133.6 (12499)	309.5 (2074)	200.9 (1346)	19	11	1.2	12.3 $\pm$ 0.2 (108)	358.5 $\pm$ 15.6
					<i>Baikal/Patom Ranges</i>							
BA02	Gneiss	N55°43'13.7"/E109°28'38.4"	462	19	110.1 (10714)	22.9 (120)	31.5 (165)	4	95	0.2	13.6 $\pm$ 0.4 (11)	142.1 $\pm$ 17.2
BA03	Granite	N55°46'27.4"/E109°33'24.9"	481	19	111.9 (10714)	100.2 (410)	117.8 (482)	15	100	1.4	13.3 $\pm$ 0.2 (57)	168.6 $\pm$ 11.6
BA04	Gneiss	N55°40'14.5"/E109°24'40.0"	469	20	107.1 (10714)	234.6 (875)	203.5 (759)	23	1	10.5	13.8 $\pm$ 0.3 (26)	217.9 $\pm$ 11.3
BA05A	Gneiss	N55°45'08.3"/E109°17'11.7"	582	20	104.8 (10714)	227.9 (1926)	309.1 (2612)	37	41	2.3	12.5 $\pm$ 0.1 (133)	137.2 $\pm$ 4.7
BA05B	Gneiss	N55°45'08.3"/E109°17'11.7"	582	16	97.7 (10714)	158.2 (1038)	197.7 (1297)	27	93	0.0	13.7 $\pm$ 0.1 (112)	138.8 $\pm$ 6.2
BA07	Granite	N55°45'32.4"/E108°48'31.0"	951	19	130.2 (12499)	75.5 (629)	156.5 (1304)	17	50	1.2	13.2 $\pm$ 0.2 (80)	111.4 $\pm$ 5.9
BA08	Granite	N55°44'17.5"/E108°44'05.2"	751	19	102.4 (10714)	123.0 (898)	172.1 (1189)	21	93	3.4	13.0 $\pm$ 0.2 (103)	137.3 $\pm$ 6.4
					<i>Barguzin Range</i>							
b1	Granite	N53°36'01.7"/E109°27'01.7"	1676	20	106.1 (9963)	86.4 (654)	315.3 (2387)	36	32	1.4	13.4 $\pm$ 0.1 (102)	48.5 $\pm$ 3.6
b2	Granite	N53°35'49.3"/E109°27'05.3"	1571	19	110.7 (9963)	114.0 (759)	374.2 (1492)	41	68	2.8	13.3 $\pm$ 0.1 (100)	56.4 $\pm$ 3.9
b3	Granite	N53°35'38.2"/E109°27'22.7"	1457	20	102.6 (9963)	50.8 (622)	181.1 (2218)	20	53	0.6	13.5 $\pm$ 0.1 (102)	48.2 $\pm$ 3.5
b4	Granite	N53°35'30.8"/E109°27'34.6"	1371	20	107.2 (9963)	47.7 (629)	159.3 (2099)	18	17	1.6	13.2 $\pm$ 0.1 (101)	54.0 $\pm$ 4.0
b5	Granite	N53°35'18.8"/E109°27'42.0"	1282	19	101.4 (9963)	118.0 (879)	358.4 (2670)	43	6	3.1	12.9 $\pm$ 0.2 (105)	55.9 $\pm$ 3.8
N13	Granite	N53°56'18.7"/E109°54'02.5"	1844	25	108.4 (10796)	31.27 (404)	117.3 (1516)	13	57	0.5	12.4 $\pm$ 0.2 (104)	48.4 $\pm$ 3.8
N14	Granite	N53°56'07.2"/E109°54'14.3"	1740	20	108.0 (10796)	63.65 (464)	200.7 (1463)	21	95	0.3	12.2 $\pm$ 0.1 (101)	57.3 $\pm$ 4.4
N25	Granite	N53°56'02.4"/E109°56'24.0"	900	19	116.5 (9963)	112.9 (1065)	632.4 (5964)	68	9	2.1	11.8 $\pm$ 0.2 (100)	34.9 $\pm$ 2.3
O13	Granite	N53°55'58.8"/E109°56'35.2"	800	16	113.0 (9963)	100.2 (416)	570.4 (2367)	75	23	2.4	11.6 $\pm$ 0.2 (101)	33.9 $\pm$ 2.8
W1	Granite	N54°33'26.8"/E110°24'32.9"	2153	20	118.8 (9963)	17.07 (198)	61.9 (718)	6	95	0.0	12.1 $\pm$ 0.4 (23)	57.2 $\pm$ 4.6
W2	Granite	N54°33'14.1"/E110°24'27.0"	1968	25	107.3 (10796)	21.1 (275)	80.8 (1051)	9	23	0.2	12.1 $\pm$ 0.2 (40)	47.8 $\pm$ 4.6

<sup>a</sup>Alt is the sampling altitude in m; Nb is the number of crystals analyzed;  $\rho_d$  is the CN5 glass dosimeter induced track density per  $\text{cm}^{-2}$  (number in parentheses is the total number of tracks counted);  $\rho_s$  and  $\rho_t$  represent sample spontaneous and induced track densities per  $\text{cm}^{-2}$  (number in parentheses is the total number of tracks counted); [U] is the calculated uranium density (in ppm);  $P(\chi^2)$  is the probability in % of  $\chi^2$  for  $v$  degrees of freedom (where  $v$  is number of crystals minus 1); Var is the age dispersion in %; MTL is the measured mean fission track length in  $\mu\text{m}$ ; error is  $1\sigma$  (number in parentheses is the total number of tracks measured); FT age is the apatite fission track age in Ma (the pooled age is used when  $P(\chi^2) < 10\%$  and the central age is used when  $P(\chi^2) > 10\%$ ). Ages have been calculated using the Trackkey software [Dunkl, 2002]. Error is  $\pm 2\sigma$ .

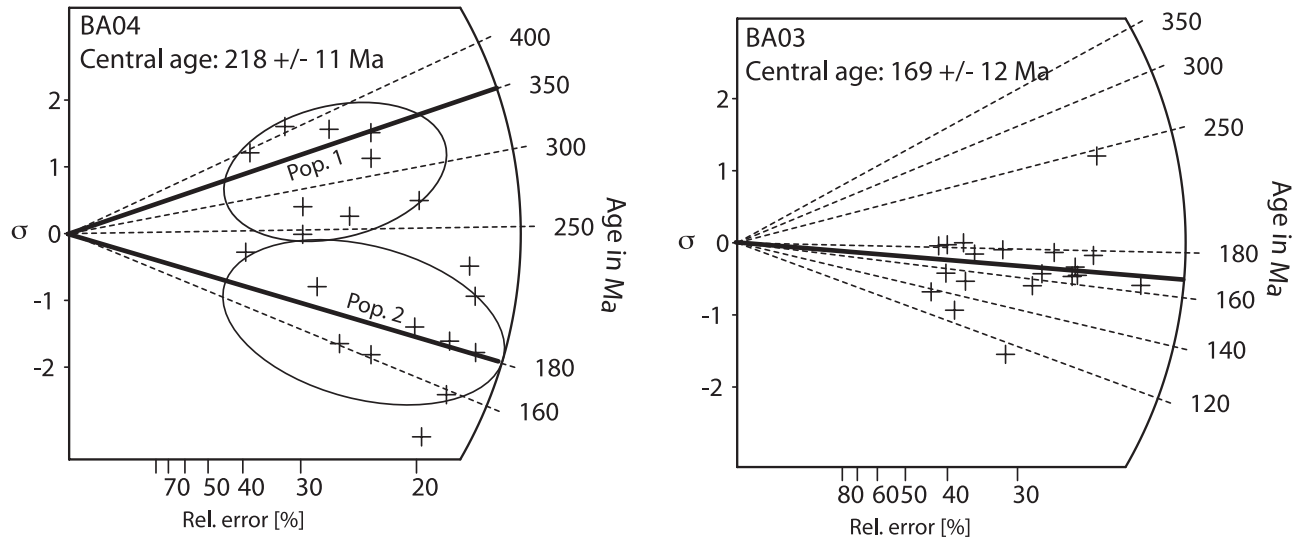


**Figure 3.** Radial plots for samples BA04 and BA03. The individual grain ages in sample BA04 can be roughly grouped in two distinct populations (circles) with respective mean ages of 350 Ma and 180 Ma (black lines). For comparison, the individual ages in sample BA03 are grouped within a single, consistent population (except for one point with an age of about 250 Ma which we do not explain). See text for further discussion on these ages.

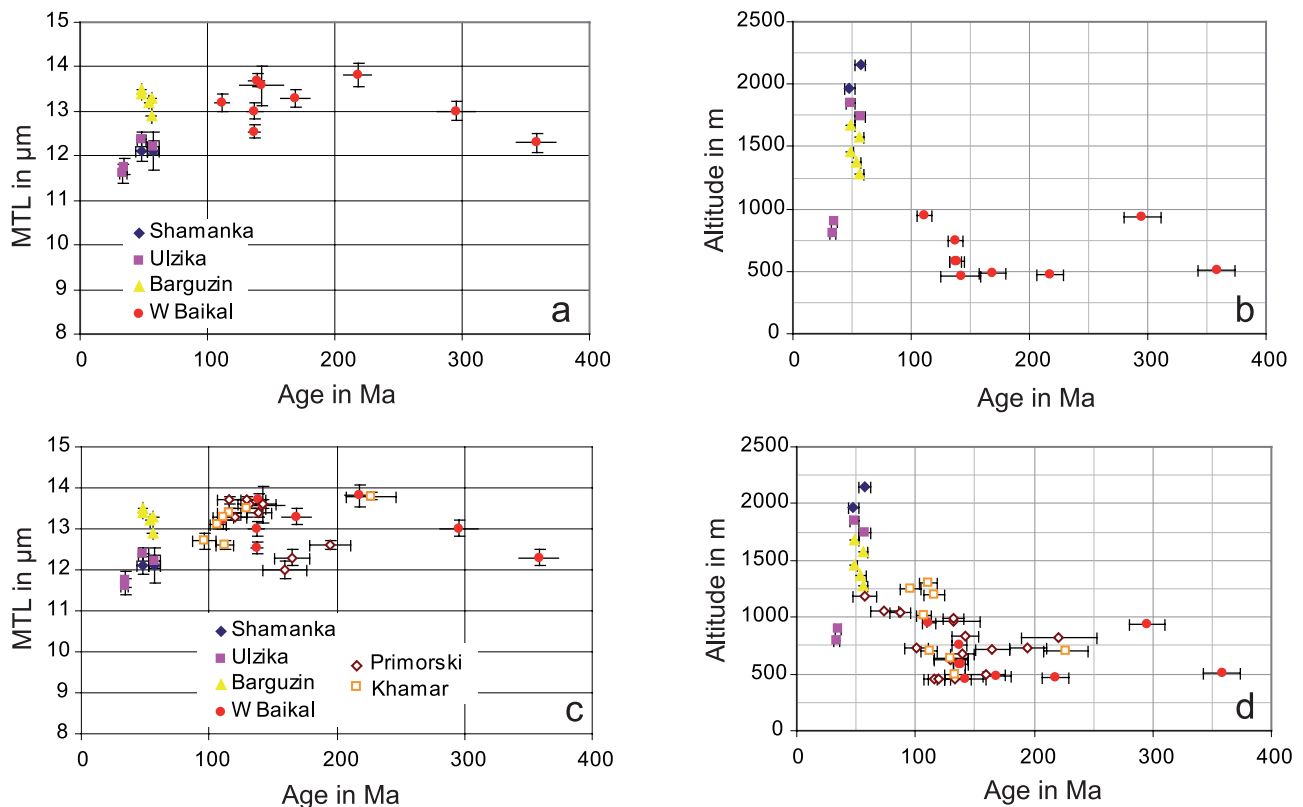


**Figure 4.** Different plots of the fission track data showing the relationships between (a and c) the mean fission track lengths (MTL) and the fission track ages and (b and d) the sampling altitude and the fission track age. Figures 4a and 4b are only considering data from this study. Figures 4c and 4d include data from *van der Beek et al. [1996]* that complete the data set for the southern part of the Baikal zone. Both sets of samples are coherent on the two types of graphs. See Table 1 in this study and Tables 1 and 2 of *van der Beek et al. [1996]* for a complete description of the data.

Siberian platform

Baikal / Patom ranges

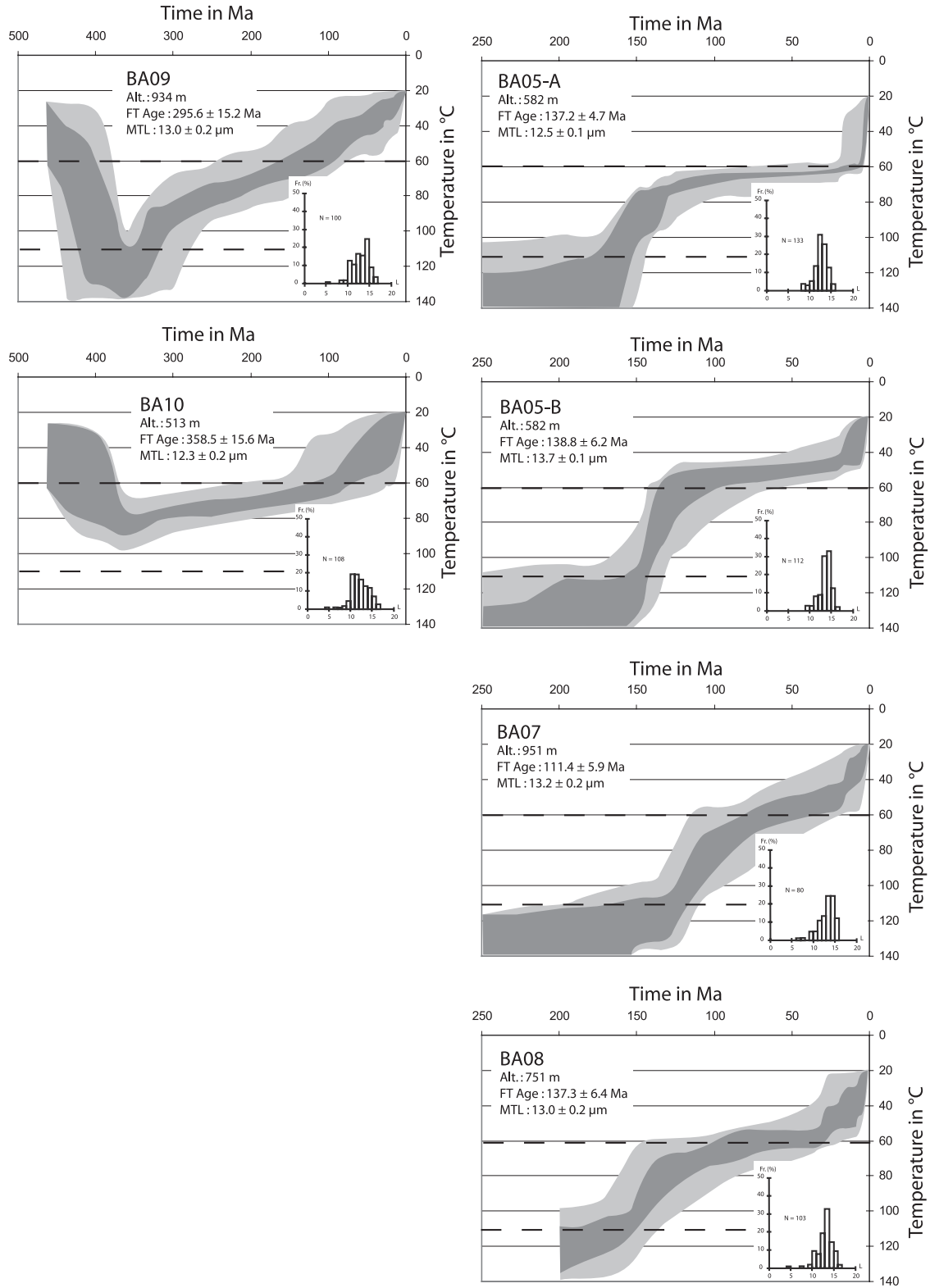


Figure 5a

rate decreases and sample BA09 slowly cools down until reaching 60°C between late Jurassic and early Cretaceous times. Sample BA10 remains at temperatures not exceeding 90°C at the end of the subsidence stage. From the late Devonian, sample BA10 also displays a slow, regular cooling, which brings it to the upper part of the PAZ (60°C) in early Upper Cretaceous times. The model does not constrain the final cooling of the sample.

[34] Modeling of fission track data provides a temperature versus time evolution of samples BA09 and BA10 that reflects burying and exhumation periods. However, it does not give any direct indication on the vertical position of these samples within the sedimentary section. In order to estimate the amount of sediments deposited on samples BA09 and BA10, we used the thermal history provided by the fission track data as a reference and independently computed the depth/temperature evolution of these samples, taking into account both thermal diffusion and advection such as:

$$\frac{dT}{dt} = \kappa \frac{d^2T}{dz^2} - u \frac{dT}{dz}$$

where  $T$  is the temperature,  $t$  is the time in seconds,  $z$  is the depth,  $\kappa$  is the thermal diffusivity, and  $u$  is the advection velocity (in  $\text{m s}^{-1}$ ), negative downward (Figure 6). The initial (before subsidence) thermal gradient is a steady state geotherm for the cratonic crust with a low surface heat flow of  $45 \text{ mW m}^{-2}$ . This thermal gradient is then modified during calculation to take into account the advection of material. With those initial conditions, we assume that both samples are located  $\sim 1000 \text{ m}$  beneath the surface, i.e., at a temperature of about 40°C, which corresponds to the mean starting point of the AFT model. We then use a trial-and-error method to compute the temperature-time evolution of both samples until it fits the one predicted by AFT track length models. Best fitting models show that sample BA09 has been buried beneath 4800 m of sediments between its initial location at 460 Ma and its greater depth around 365 Ma. This corresponds to a subsidence rate of  $0.05 \text{ mm a}^{-1}$ . Conversely, sample BA10 is only covered by 2300 m of sediments during the same time span, which gives a much lower subsidence rate ( $0.024 \text{ mm a}^{-1}$ ). Therefore, around 365 Ma the two samples were vertically offset by about 2500 m.

[35] From the late Devonian, sample BA10 displays a slow, regular cooling which brings it to the upper part of the

PAZ (60°C) in early Upper Cretaceous times. The model does not constrain the final cooling of the sample.

[36] Sample BA09 crosses the 110°C isotherm between 350 and 320 Ma (early Carboniferous). Between 320 and 300 Ma the cooling rate decreases and sample BA09, like sample BA10 slowly cools down until reaching 60°C between late Jurassic and early Cretaceous times.

### 3.4. Low-Temperature Evolution of the Baikal Range

[37] Because of the small number of horizontal fission tracks that could be measured, samples BA02, BA03, and BA04 were not modeled. Samples BA08, BA05A, and BA05B (Figure 5a and Table 1) present a rapid cooling event starting between 170 and 150 Ma and ending around 120–110 Ma when the samples either cross the upper limit of the PAZ (BA05B) or continue to cool slowly toward the surface. Sample BA07 (Figure 5a and Table 1), younger in age but higher in altitude enters the PAZ later, between 130 and 120 Ma suggesting either differential vertical movements between the three samples, a stronger or a later exhumation in the axial zone of the range. The thermal history of sample BA07 indicates that the rapid cooling event ends around 100 Ma and is followed by a period of slower cooling that can be associated with erosion.

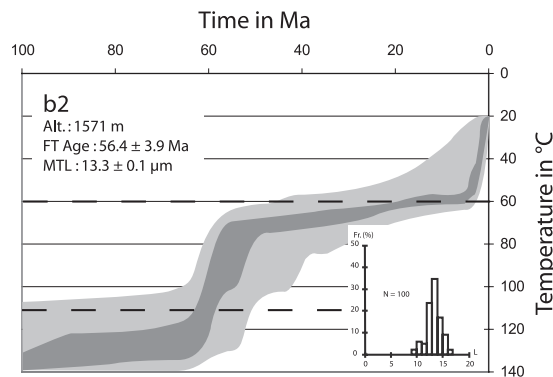
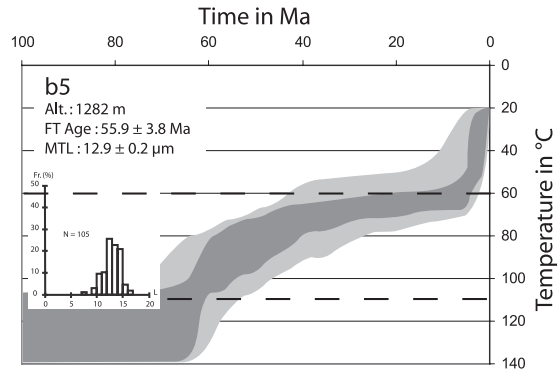
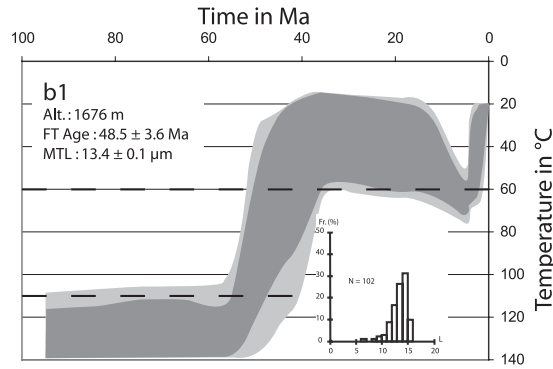
### 3.5. Low-Temperature Evolution of the Barguzin Range

[38] Samples b1 to b5 from the Barguzin profile (near the mouth of the Barguzin basin toward the Centre Baikal basin) cross the 110°C isotherm between 65 and 50 Ma during an episode of rapid cooling which probably brings all the samples to the near surface (Figure 5b). Sample b5, located at the lowest altitude in the profile remains in the PAZ until late Miocene–early Pliocene times and seems to cool rapidly around 5 to 10 Ma. This last cooling event is also recorded in other samples from this profile (b4, b3, and b1) following a period of reheating possibly up to  $\sim 70^\circ\text{C}$  after the Eocene cooling (Figure 5b). However, because it occurred at temperatures close to the upper limit of the PAZ, the Mio-Pliocene exhumation is not well constrained in those last three samples.

[39] Samples from the Ulzika profile (Figure 5c) display the same initial cooling event as samples from the southern profile. Sample N13 located on top of the profile enters the PAZ around 65 to 60 Ma. Sample N14 located below N13 crosses the 110°C isotherm slightly earlier (around 75 to 65 Ma), but this, like its older fission track age, might be an artifact of the model due to the different chemical

**Figure 5a.** Reverse modeling of apatite fission track lengths for samples from the Siberian platform and the Baikal-Patom range. Models were obtained using the AFTSolve<sup>®</sup> software [Ketcham *et al.*, 2000]. Alt is the sampling altitude, FT age is the fission track age (see Table 1), and MTL is the measured mean track length. The dark gray area represents the envelope of all the possible temperature-time curves falling within a  $1\sigma$  error interval from the best fit curve. The light gray area represents the envelope of all the cooling curves falling within a  $2\sigma$  interval. Only the area between 110°C and 60°C (designed as partial annealing zone or PAZ, between the dashed lines on the graphs) is representative. The track lengths histogram is displayed for each sample. L is the track length in  $\mu\text{m}$ , Fr (%) is the frequency of measurements in %, and N is the total number of tracks measured. For clarity, reasons the time scale (horizontal) of the temperature-time models varies between the various groups of samples. See text for discussion of the graphs.

Barguzin range ( Barguzin profile)



Barguzin range ( Shamanka profile)

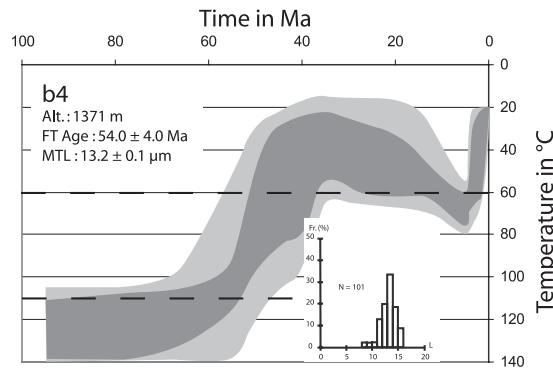
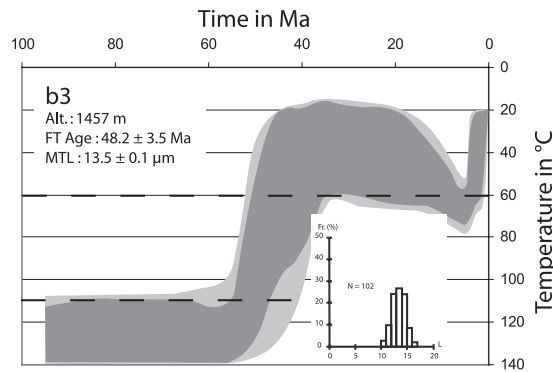
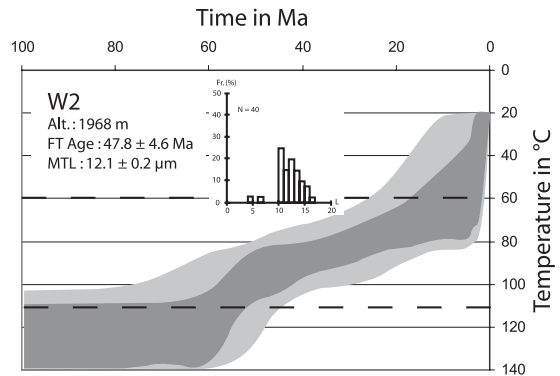
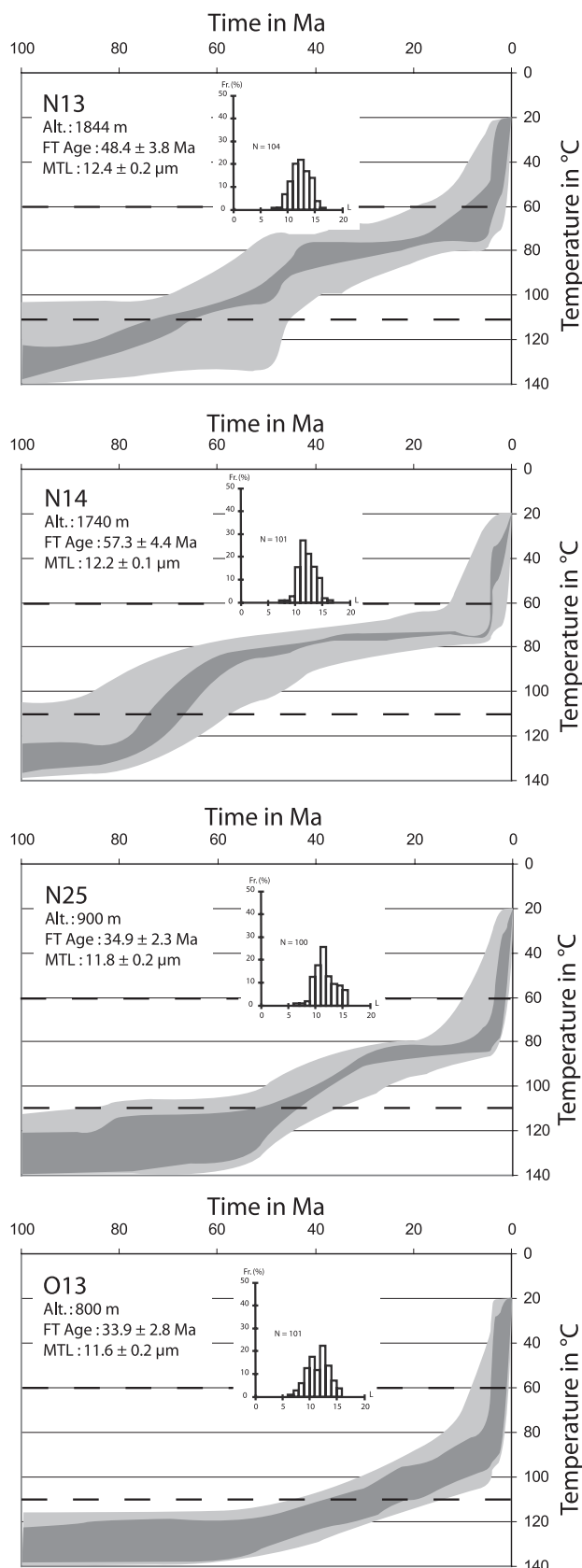


**Figure 5b.** Reverse modeling of apatite fission track lengths for samples from the Barguzin range (Barguzin and Shamanka profiles). See Figure 5a for key.

## Barguzin range (Ulzika profile)



composition of this sample. On the lower part of the profile, sample N25 enters the PAZ between 50 and 45 Ma, and sample O13 between 40 and 30 Ma. After this initial Eocene to early Oligocene cooling, all the samples (except O13, which is exhumed later because of its position at the bottom of the section) remain in the PAZ between 90 and 80°C and then reach the surface during a rapid cooling event (60 to 70°C in 5 Ma) clearly identified around 5 Ma. This last cooling event is also recorded in sample O13 by a strong increase of the cooling rate. Considering a mean geothermal gradient of 30°C per kilometer, samples N25 and O13 are brought toward the surface at a mean rate of  $\sim 0.4$  to  $0.45$   $\text{mm a}^{-1}$  within the last 5 Ma and at then  $0.03$   $\text{mm a}^{-1}$  between 30 Ma and 5 Ma.

[40] Sample W1 from the Shamanka profile was not modeled because of the small number of horizontal fission tracks that could be measured (Table 1). Sample W2 (Figure 5b and Table 1) is also poorly constrained with only 40 track lengths measurements. However, it displays the same thermal history as samples from the Ulzika profile: a first episode of rapid cooling starting around 60 to 50 Ma followed by a period of slow cooling from late Eocene to late Miocene times and finally a renewed exhumation starting around late Miocene–early Pliocene times.

## 4. Discussion

### 4.1. Paleozoic Relief Building in the Baikal and Patom Ranges

[41] On the Siberian platform, samples BA09 and BA10 experience continuous sediment burying from their Early Ordovician deposition age to the Late Devonian–Early Carboniferous (Figure 5a). By that time (circa 360–350 Ma) sample BA10 collected well inside the platform is covered by about 3 km of sediments whereas sample BA09 located closer to the Baikal and Patom ranges is covered by about 4 km of sediments (Figure 6). This  $\sim 100$  Ma subsidence episode is coeval with the beginning of accretion of the remote Tuva–Mongolia (Late Cambrian–Early Ordovician) and Khamar–Daban blocks (Late Silurian–Early Devonian) [Fedorovskii *et al.*, 1993; Zorin *et al.*, 1993; Gibsher *et al.*, 1993; Delvaux *et al.*, 1995a; Gusev and Khain, 1996] and predates the onset of compressional deformation in the outer Patom region [de Boisgrollier *et al.*, 2009].

[42] Given the relatively wide distribution of Ordovician detrital sediments, the volume of eroded material may have been important, which would suggest strong and/or widespread topography to the east and south. The lack of an unconformity or any other indication of synsedimentary deformation in the basin indicates that the tectonic effects of the collisions to the south did not affect the basin which was probably far from the mountain range.

**Figure 5c.** Reverse modeling of apatite fission track lengths for samples from the Barguzin range (Ulzika profile). See Figure 5a for key.

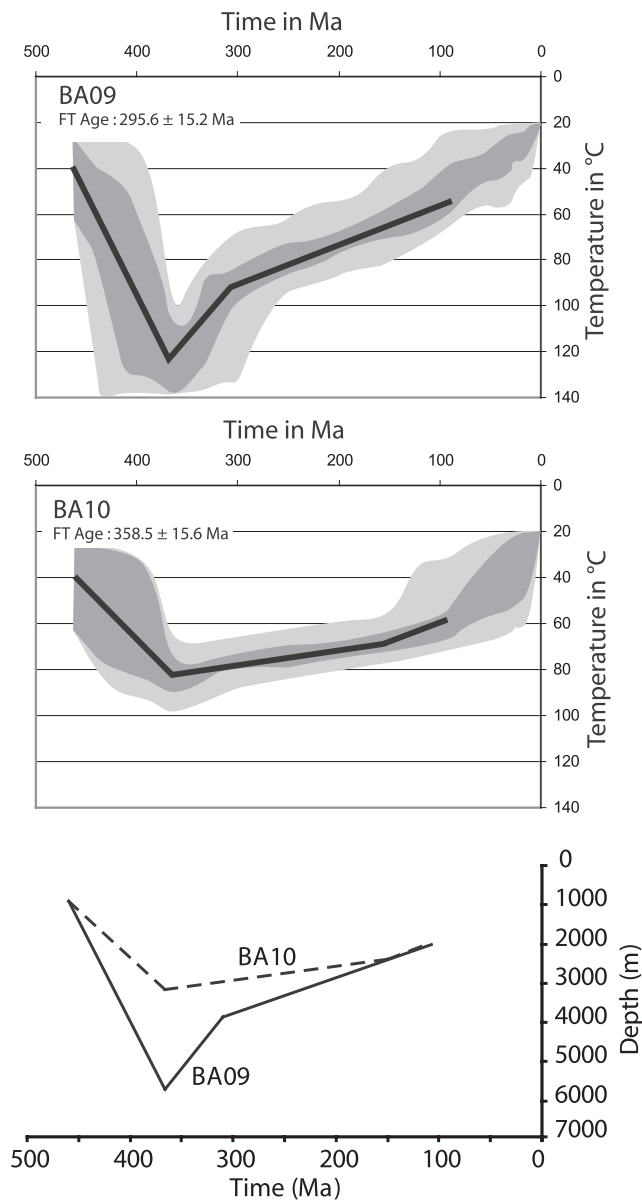


**Figure 6.** Model of depth evolution history for the Ordovician detrital samples BA09 and BA10 from the Siberian platform. Depth versus time paths are computed using the mean temperature time path calculated using fission track data (Figure 5a and Table 1) and taking into account both thermal diffusion and advection. See text for discussion of the models and results.

[43] The thermal history derived from track lengths modeling implies that burying stopped and exhumation started around Early Carboniferous (350–320 Ma). This change in thermal history is particularly well imaged on sample BA09, which crosses the 110°C isotherm with a relatively rapid cooling rate, which then decreases around the Upper Carboniferous (320–300 Ma) (Figures 5a and 6). This cooling episode can be associated with the closure of

the Paleo-Asian ocean in the Carboniferous (Figure 7), which induced folding and thrusting in the Baikal and Patom belts. The rapid cooling rate recorded by sample BA09 in the Early Carboniferous indicates that this deformation affected the Ordovician, Silurian and Devonian sediments of the Siberian platform. Sample BA10 does not display that initial rapid cooling phase, suggesting that the Carboniferous deformation was less important in the outer domain than at the front of the Baikal-Patom range.

[44] Finally, the thermal history of samples BA10 and BA09 indicates that if subduction along the southern margin of the Dzhida, Khमार Daban-Barguzin, and Stanovoy blocks initiated in Late Silurian–Early Devonian, deformation and relief building of the sedimentary cover of the Angara-Lena plate during Early Carboniferous is most probably related to the subsequent collision coeval to or preceding the emplacement of the Angara-Vitim batholith.

#### 4.2. Middle Jurassic–Early Cretaceous Denudation Around Lake Baikal

[45] On the Siberian platform, samples BA10 and BA09 cool slowly and regularly through the late Paleozoic, Mesozoic and early Cenozoic, reaching the upper limit of the PAZ between Jurassic and Late Cretaceous times. This very slow cooling can be related to slow, continuous erosion of the sedimentary cover.

[46] Within the Baikal range, all samples have Mesozoic ages and the four that have been modeled do not provide any indication on the pre-Mesozoic thermal history of the range (Figure 5a). These results are consistent with the data obtained by *van der Beek et al.* [1996] in the Primorsky range, the Olkhon block and the Khमार Daban mountains (Figures 2, 4c, and 4d); *van der Beek et al.* [1996] described a rapid cooling of three modeled samples (2 from the Olkhon block and 1 from the Khमार Daban Mountains) around 140–120 Ma that brought the samples from temperatures higher than 120°C to less than 60°C. They interpreted those results as the consequence of a rapid cooling episode during the Early Cretaceous, associated with the closure of the Mongol-Okhotsk ocean and the collision between the southern margin of Siberia and the Mongolia–north China block (Figure 7). Finally, they suggested that the random variation of their AFT data may be due to local variations in the geothermal gradient mostly driven by magmatic activity [e.g., *Ermikov*, 1994; *Yarmolyuk and Kovalenko*, 2001].

[47] In the Baikal range, our data indicate that the rapid cooling event starts even earlier, during the Middle Jurassic (170–150 Ma) and ends, like reported by *van der Beek et al.* [1996] during the late Early Cretaceous, around 120–110 Ma (Figure 5a). The onset of rapid cooling is contemporaneous with the change from marine to continental-derived sedimentation in the Trans-Baikal region [*Mushnikov et al.*, 1966; *Ermikov*, 1994] and with basin inversion and erosion in China and Mongolia [e.g., *Meng*, 2003], which mark the onset of the Mongol-Okhotsk orogenesis. Unlike the data presented by *van der Beek et al.* [1996] the mean fission track ages of our samples are very consistent across the Baikal range (Figure 2 and Table 1) and display (1) an abrupt change in ages between the Siberian platform and the

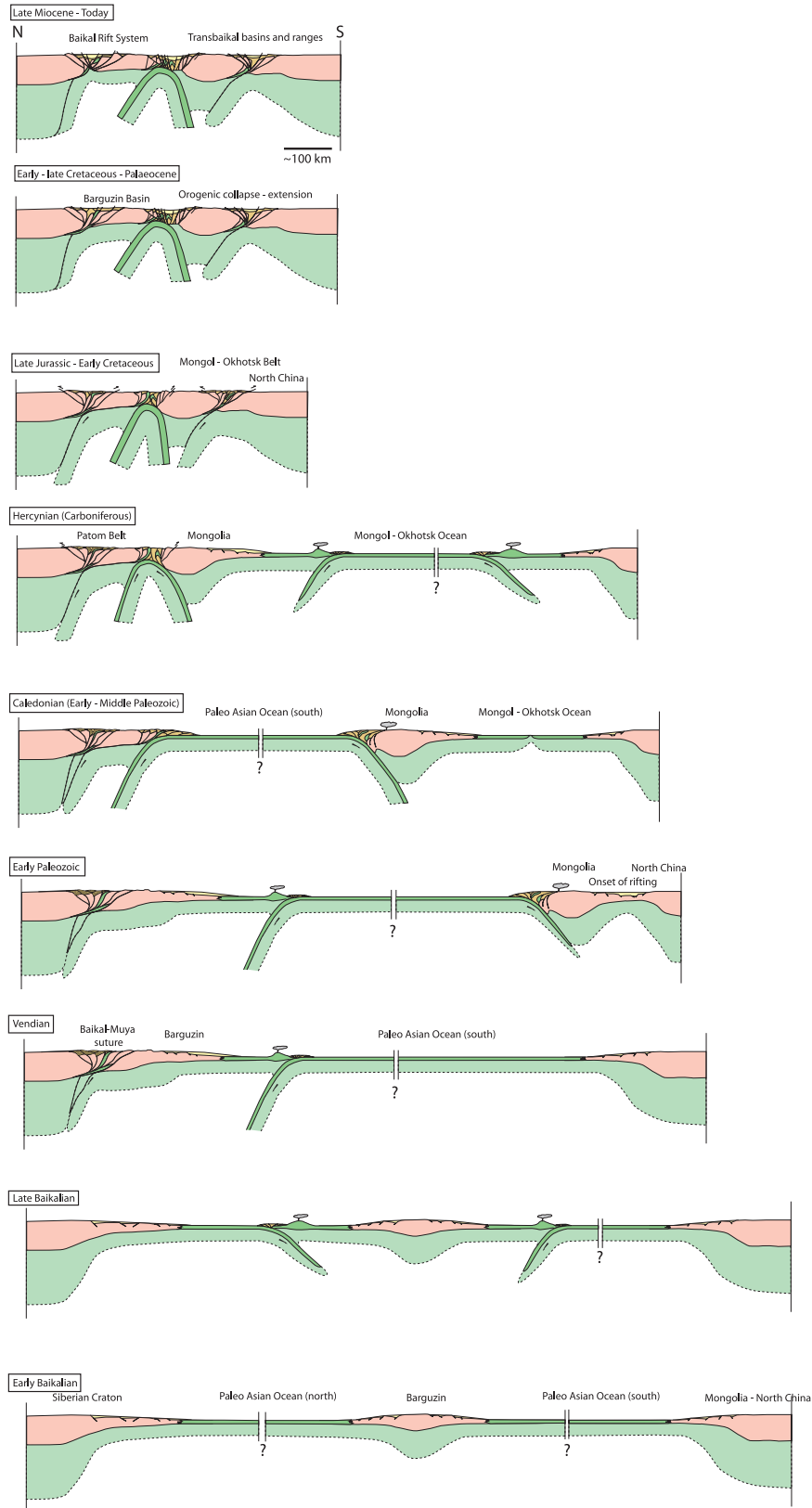


**Figure 7.** Synthetic cross sections showing the tectonic evolution of SE Siberia and NE Mongolia from the Siberian craton to Mongolia across the actual BRS, Barguzin block and Mongol-Okhotsk belt. Only the major blocks have been identified. See text for discussion of the main tectonic events.

range, corresponding to the sharp step in the morphology along the West Patom Thrust; (2) ages of  $137 \pm 5$  Ma and  $139 \pm 6$  Ma on the “external” parts of the range; a younger age of  $111 \pm 6$  Ma (sample BA07) in the central part of the range; and (3) older ages of  $169 \pm 12$  Ma and  $218 \pm 11$  Ma immediately near Lake Baikal.

[48] Modeling of sample BA07 (Figure 5a) shows that it crosses the  $110^\circ\text{C}$  isotherm around 130–120 Ma later than the other samples from the Baikal range, and would thus have a thermal history similar to the samples analyzed by *van der Beek et al.* [1996]. The younger age obtained for sample BA07 (Table 1) implies either weaker erosion in that part of the range if sample BA07 comes from a depth similar to the others samples, or differential movements along internal structures during the formation of the relief. The internal part of the range is presently a region of high topography. If the situation was similar during the Mesozoic then we should consider that erosion may have effectively been higher in the central part of the range, therefore, that sample BA07 was exhumed from deeper levels than the other samples. Indeed, sample BA07 was collected very close to the Paleozoic North Baikal Fault (Figure 2), which may have been reactivated as a thrust fault during the Mesozoic deformation episode, leading to differential exhumation within the range. This second hypothesis explains the later onset of cooling for sample BA07 but also the fact that cooling of this sample ended slightly later than for the others.

[49] Unlike west of the Baikal range, there is no sharp morphological step between the samples located near the shore of Lake Baikal and those of the “external” part of the range to the east (not considering the steep Cenozoic normal faults) (Figure 2). Still, there is a change in fission track ages implying that the samples located close to the lake have been less affected by the Middle Jurassic–Early Cretaceous cooling. This favors the hypothesis of a reactivation of the North Baikal Fault, which induced renewed exhumation close to the fault and low-relief building associated with low erosion near the present-day lake.

[50] Relief building around Lake Baikal thus starts in the Middle Jurassic in relation with the Mongol-Okhotsk orogeny to the SE. In the Baikal range, relief building is limited to the west by the West Patom Thrust (Figure 2) on which is located the present morphological step between the range and the Siberian platform. Inside the range, the North Baikal Fault is most probably reactivated leading to eastward tilting of the eastern part of the range and differential relief building and exhumation. Cooling due to the activity of this fault (relief building and associated erosion) lasts until circa 100 Ma.

[51] Building of a wide relief in the Baikal–southern Patom ranges is contemporaneous with the large-scale extension that follows the closure of the Mongol-Okhotsk ocean SE of the Baikal-Vitim terrane and down to Mongolia and China [e.g., *Zheng et al.*, 1991; *van der Beek et al.*, 1996; *Davis et al.*, 1996, 2001, 2002; *Webb et al.*, 1999; *Zorin*, 1999; *Darby et al.*, 2001b; *Meng*, 2003; *Fan et al.*, 2003; *Wang et al.*, 2006]. However, the sharp change in fission track ages across the topographic step corresponding

to the West Patom Thrust clearly indicates that this fault has been reactivated during the relief building episode. As there is no evidence of normal motion on that fault [*Delvaux et al.*, 1995a, 1997], the Mesozoic West Patom fault was most probably a thrust fault. Similarly, movement along the North Baikal Fault and eastward tilting of the eastern block suggest a reverse motion on this fault.

[52] The fate of the sediments that are generated during the Middle Jurassic–Early Cretaceous erosion stage remains unsolved. Our fission track data indicate that if any, only a thin (less than a few hundreds meters) sedimentary cover can have been deposited on the Siberian platform to the west. Fission track data from *van der Beek et al.* [1996] show that during Early Cretaceous, the SW and SE borders of the Baikal rift were submitted to erosion, which precludes any possibility for sedimentation in that area. Farther to the west on the platform and to the south in the Sayan–Angara there is no indication of Late Jurassic or Cretaceous sediments. The only potential sedimentation areas are the Vilui basin north of the Patom belt and the Arctic Ocean. Sediments eroded from the Baikal and Patom ranges would have been transported by a river system similar to the actual Lena and Vitim systems. This hypothesis suggests that the river network remains very constant across Late Mesozoic and Cenozoic times [*Prokopyev et al.*, 2008].

#### 4.3. Late Cretaceous to Quaternary Evolution of the Barguzin Range and Basin

[53] Similar to the samples analyzed by *van der Beek et al.* [1996], our data obtained in the Baikal ridge do not provide any indication on the Cenozoic thermal history of the area (Table 1 and Figure 5a). All of them either cross the  $60^\circ\text{C}$  isotherm shortly after the Middle Jurassic–Early Cretaceous event or slowly cool down toward the surface with no marked thermal event. This is consistent with the paleogeographic reconstruction of *Mats et al.* [2001]: from Paleocene to early Oligocene times, the present-day Baikal range, north Baikal depression and Patom region are occupied by a “slightly elevated” denudation plateau with Mesozoic inherited reliefs and covered by a laterite-kaolinite weathering crust.

[54] The results are very different in the Barguzin area (Figure 2), in which only Cenozoic ages are found (Table 1). Fission track lengths modeling provide a complete thermal history of the eastern side of the Barguzin range from late Late Cretaceous to Quaternary (Figures 5b and 5c).

[55] The Barguzin basin (Figure 2) belongs to the BRS and is limited to the northwest by a series of SW–NE directed en echelon active normal faults that separate the basin (~500 m high) from the up to 2600 m high Barguzin range (Figure 2) [e.g., *Florensov*, 1960; *Solonenko*, 1968, 1981; *Delvaux et al.*, 1997; *Epov et al.*, 2007; *Lunina and Gladkov*, 2007]. To the east, the basin is separated from the Ikat mountains by another set of small-offset SW–NE normal faults. The basin infill is asymmetric with a greater sediment thickness (up to 2.5 km) on its western side near the Barguzin range [e.g., *Solonenko*, 1981; *Nevedrova and Epov*, 2003; *Epov et al.*, 2007]. A borehole within the

central Barguzin basin crossed the entire Quaternary and Cenozoic series and reached the basement at 1400 m [Florensov, 1982]. The oldest recognized sediments are middle Pliocene clay siltstones and sandstones. Sarkisyan [1958] and Florensov [1960] inferred the existence of a Miocene lake within the basin, but no Miocene sediments have been identified. The recognized upper Pliocene section is made of conglomerates and sandstones. Finally, the Quaternary series are made of unconsolidated conglomerates, gravels, sandstones and siltstones. Several blocks of uplifted basement have been identified within the basin [Florensov, 1960; Nevedrova and Epov, 2003; Epov et al., 2007]. From sedimentary data, the evolution of the Barguzin basin started during middle Pliocene times when the “fast rifting” stage initiated in the Baikal rift. The apatite fission track data presented in this work are consistent with the occurrence of a Pliocene phase in the evolution of the basin, and also account for a much longer history.

#### 4.3.1. Late Cretaceous–Eocene

[56] Along the three profiles of the Barguzin basin, all samples located now at the highest altitude cross the 110°C isotherm between about 65 Ma and about 50 Ma during a phase of rapid cooling (Figures 5b and 5c). This event appears more strongly marked in the Barguzin profile, south of the Barguzin range, where most samples reach the near surface by Eocene times. The other samples do not reach the near surface but remain in the apatite PAZ (b5, N13, N14, or W2) and record a period of slow cooling after the Eocene.

[57] The stronger exhumation in the south of the basin (Barguzin profile) (Figure 5b) cannot be driven by external processes such as different climate conditions leading to stronger erosion, because the distance between the profiles is too small. It is thus interpreted as the result of differential tectonic uplift between individual basement blocks separated by the SW–NE faults mapped within the Barguzin range.

[58] On the basis of sediment analysis, the onset of rapid rifting in the Tunka, north Baikal and central Baikal basins is dated around late Oligocene–Miocene [e.g., Mats, 1985, 1993; Mats et al., 2001; Logatchev, 1993, 2003; Petit and Déverchère, 2006]. However, Late Cretaceous–Eocene sediments are found in and around the Tunka and north Baikal basins [Mats, 1993; Scholz and Hutchinson, 2000]. A precursor of the South Baikal Depression started to form in Late Cretaceous–early Paleocene [Tsekhovskiy and Leonov, 2007]. To the SE, in the southern Vitim area, small grabens such as the Eravna basin contain Late Cretaceous clastic sediments known as the Mokhei Formation [Rezanov, 2000; Skoblo et al., 2001; Tsekhovskiy and Leonov, 2007]. These sediments rest with an erosional contact on the Cretaceous kaolinic weathering crust. Rezanov [2000] indicates that during the Paleogene, the northern edge of the Eravna depression was bordered by reliefs while its southern edge was connected with a planation surface.

[59] The strong cooling event recorded by apatite fission track analysis implies that exhumation in the Barguzin range started in the Late Cretaceous. We suggest that this uplift was accommodated, like in the present-day, by vertical motions on the Barguzin fault, though the absence

of fission track data east of the Barguzin basin does not allow confirming this hypothesis. In this case, the Barguzin fault could have been in the continuity of the large offset Morskoy fault that bounds the central Baikal basin [e.g., Hutchinson et al., 1992; Petit and Déverchère, 2006].

[60] The extension that was thought to be restricted to the southern and central Baikal zone and the Vitim area until Oligocene times thus probably reached the northern Barguzin basin in the Late Cretaceous–Paleocene (Figure 7). South of the Barguzin basin, extension was probably localized in the South Baikal Depression [Tsekhovskiy and Leonov, 2007].

[61] The results of van der Beek et al. [1996] do not show any evidence of late Late Cretaceous–Paleocene denudation NE of the Selenga delta, in the Khमार Daban range. The present-day topography of this area is much lower than that of the Barguzin range, and no large extensional basins are present (Figure 2). The Late Cretaceous–Paleocene extensional deformation thus appears to have been localized on areas relatively similar to the late Tertiary–Quaternary deformation.

[62] The initiation and development of the Baikal rift zone is generally thought to be either the surface effect of a wide asthenospheric diapir beneath the rift axis [e.g., Zorin, 1981; Windley and Allen, 1993; Logatchev and Zorin, 1987; Gao et al., 2003; Zorin et al., 2003; Johnson et al., 2005; Kulakov, 2008] or more frequently a direct consequence of the far-field effects of the collision between India and Asia farther south [e.g., Molnar and Tapponnier, 1975; Tapponnier and Molnar, 1979; Delvaux et al., 1997; Petit et al., 1996; Petit and Déverchère, 2006]. Alternative models explain the initiation and development of the Baikal rift by complex interactions between the India–Asia collision and the Pacific–east Asia subduction associated to prerift crustal heterogeneities inherited from the long-lasting tectonic history of the region [e.g., Delvaux, 1997].

[63] If extension does initiate in the Barguzin area during the late Late Cretaceous, prior to the India–Asia collision [e.g., Patriat and Achache, 1984; Besse et al., 1984; Patzelt et al., 1996; Ali and Aitchison, 2006] the driving mechanism of this initial stage cannot be related to the far-field effects of this collision. As most rift-related volcanism is younger than the Paleocene (S. V. Rasskasov et al., presented paper, 2002), asthenosphere-driven extension is unlikely too. An alternative explanation is that a mechanism similar to the one responsible for the Late Jurassic–Early Cretaceous general extension in the Transbaikal region was still active in the Late Cretaceous and induced the structuring of the Barguzin range and basin, like in the Eravna depression ~10 Ma before. This transitional stage was followed by a “true rifting” stage during which some of the old depressions were rejuvenated (north and Centre Baikal, Barguzin), others were abandoned (Eravna) and new ones were created (north Baikal basins). Rassakov [1993] proposed that during late Oligocene–early Pliocene, the variations of the stress field in the eastern Baikal Rift Zone might be linked to the Pacific–east Asia active margin. Delvaux [1997] also suggested that compressive intraplate stress field generated by the Pacific–east Asia

subduction zone during Oligocene-Miocene times may be at the origin of the “slow rifting” stage.

#### 4.3.2. Oligocene

[64] The Paleocene-Eocene rapid cooling event recorded by the apatite fission track data is followed by a period of very slow cooling for the samples located in the upper part of the profiles (samples N13, N14, b5, W2 (Figures 5b and 5c)). By that time those samples are only submitted to erosion and no more to tectonic exhumation. Simultaneously, the samples located in the lower part of the profiles (N25 and O13) continue to be exhumed both through erosion and tectonic denudation (Figure 5c). Sample N25 located at 900 m cools down to  $\sim 85^{\circ}\text{C}$  by early–middle Oligocene and then stops cooling. Sample O13 located lower down at 800 m crosses the  $110^{\circ}\text{C}$  isotherm around 35 to 30 Ma (early Oligocene). This cooling pattern implies a rapid, tectonic denudation of the lowest samples while the uppermost samples, rapidly exhumed previously, are only submitted to slow cooling through erosion. We interpret it by the progressive exhumation of the samples along a continuously active normal fault. The fact that cooling rates strongly decrease after the initial cooling that brings the samples within the apatite PAZ indicates that surface erosion was probably very low. This, in turn, implies that the relief created in the Barguzin range was mostly preserved and that sediment flux within the Barguzin basin may have been limited. This is consistent with the low sedimentation rates observed in the north and central Baikal basins during the same period [e.g., *Nikohyev et al.*, 1985; *Moore et al.*, 1997; *Levi et al.*, 1997; *Mats et al.*, 2000].

#### 4.3.3. Late Miocene–Quaternary

[65] Final cooling of the samples happens in the late Miocene–early Pliocene (i.e., around 5 Ma). A dramatic increase in cooling rate is recorded around 5 Ma by samples b5, N13, N14, and W2 located in the upper part of the three profiles (Figures 5b and 5c). The last cooling event is not strongly constrained in these samples because it takes place in the uppermost part of the apatite PAZ. On the contrary, the 5 Ma event is clearly visible on samples O13 and N25 located in the lower part of the profiles. This increase in cooling rate along the eastern margin of the Barguzin range is contemporaneous with the onset of the “fast rifting” phase in the Baikal [e.g., *Hutchinson et al.*, 1992; *Delvaux et al.*, 1997; *Petit and Déverchère*, 2006; *Mats et al.*, 2000] and the initiation of the north Baikal basin [e.g., *Hutchinson et al.*, 1992; *Delvaux et al.*, 1997; *Petit and Déverchère*, 2006] (Figure 7). At a regional scale, the early Pliocene marks the onset of renewed tectonic activity in Gobi Altay, Altay, and Sayan ranges generated by the northward propagation of the compressive stress generated by the India-Asia collision [*Delvaux et al.*, 1995b; *De Grave and Van den haute*, 2002; *Vassallo et al.*, 2007]. Pleistocene-Holocene inversion of the north Tunka basin implies that the SW–NE directed compression reaches the Baikal Rift Zone at that time [*Larroque et al.*, 2001]. The initiation of the “fast rifting” phase may thus follow an initial “lithosphere weakening” stage that initiated in the late Late Cretaceous–early Paleocene and result from the arrival of the SW–NE compression generated by the India-Asia

collision to the south. Compared to the wide Cretaceous collapse area, the present-day rift is much more localized. Therefore, if Cretaceous extension did initiate some early rift basins, only those which were favorably located and oriented could further develop during the true rifting stage. Their location close to the border of the Siberian craton is probably the key factor that controlled their long-lived development.

## 5. Conclusion

[66] The main phases of tectonic deformation and relief building recorded in the Baikal Rift Zone by apatite fission track thermochronology can be summarized as follows (Figure 7):

[67] 1. To the west, the Siberian platform experiences a continuous but slow sedimentation from at least the Early Ordovician to the Late Devonian. During that time, a maximum of about 4 km of sediments are deposited along the Baikal and southern Patom ranges. However, given the relatively wide spreading of those sediments over the platform, the volume of eroded material may have been important, which would indicate strong and/or widespread reliefs to the east and south.

[68] 2. Exhumation of the Early Ordovician series starts in the Early Carboniferous due to a continental collision that follows the subduction initiated in the Late Silurian–Early Devonian by the subduction along the southern margin of the Dzhida, Khamar Daban, Barguzin and Stanovoy blocks. The deformation front is probably located along the Baikal fault zone. No sediments associated to this tectonic phase are preserved on the platform.

[69] 3. A second phase of deformation that does not affect the Siberian platform is then recorded in the Baikal range. It starts during Middle Jurassic times, around 170–150 Ma contemporaneously with the onset of the Mongol-Okhotsk orogeny to the west. Deformation and relief building are mostly driven by reactivation of inherited faults such as the frontal Baikal fault zone and the more internal North Baikal Fault. Those movements lead to differential exhumation. This deformation and relief building episode probably ends around 100 Ma in the Baikal–southern Patom area. Like in the Carboniferous, the sediments derived from the erosion of the Jurassic–Cretaceous reliefs are not identified on the platform around the Patom range but may have been transported northward to the Vilui basin.

[70] 4. The third tectonic event is recorded in the samples from the Barguzin range. It initiates in late Late Cretaceous–early Paleocene contemporaneously with the formation farther south and SE of the South Baikal Depression or the Eravna basin. Deformation appears localized on discrete faults and probably restricted, in the Baikal Rift Zone, to the South Baikal Depression and the Barguzin basin. This Late Cretaceous–early Paleocene extension episode suggests that there has been a continuum between the orogenic collapse of the Mongol-Okhotsk belt that leads to the formation of numerous grabens toward the SE and the initiation of the Baikal Rift Zone. It also implies that

the initial driving mechanism for the formation of the Baikal Rift Zone is not a far-field effect of the India-Asia collision.

[71] 5. Finally, the apatite fission track data confirm the increase in tectonic activity in the Baikal Rift Zone around late Miocene–early Pliocene. This period is also marked by the onset of a strong compressive deformation in Goby Altay, Altay, and Sayan ranges due to the northward propagation of the compressive stress generated by the India-Asia collision. The conjunction between this new

mechanism and the initial, postorogenic extension might explain the increase in tectonic deformation in the Baikal Rift Zone.

[72] **Acknowledgments.** This work has been supported by Total. Samples from the Barguzin range were collected with partial financial support from the Siberian Branch of the Russian Academy of Science (grant IP 10.7.3) and from the Russian Fund for Basic Research (grant 08-05-00992). Constructive and detailed reviews by D. Delvaux and one anonymous reviewer have been greatly appreciated.

## References

- Ali, J. R., and J. C. Aitchison (2006), Positioning Paleogene Eurasia problem: Solution for 60–50 Ma and broader tectonic implications, *Earth Planet. Sci. Lett.*, *251*, 148–155, doi:10.1016/j.epsl.2006.09.003.
- Barbarand, J., A. Carter, I. Wood, and T. Hurford (2003), Compositional and structural control of fission-track annealing in apatite, *Chem. Geol.*, *198*, 107–137, doi:10.1016/S0009-2541(02)00424-2.
- Barry, T. L., A. D. Saunders, P. D. Kempton, B. F. Windley, M. S. Pringle, D. Dorjnamjaa, and S. Saandar (2003), Petrogenesis of Cenozoic basalts from Mongolia: Evidence for the role of asthenospheric versus metasomatised mantle sources, *J. Petrol.*, *44*, 55–91, doi:10.1093/ptrology/44.1.55.
- Bazarov, D. B. (1986), *Cenozoic of the Baikal and Western Transbaikal Regions*, Nauka, Novosibirsk, Russia.
- Belichenko, V. G., E. V. Sklyarov, N. L. Dobretsov, and O. Tomurtogoo (1994), Geodynamic map of the Paleo-Asian ocean (eastern part) (in Russian), *Russ. Geol. Geophys.*, *37*(7–8), 29–40.
- Berzin, N. A., and N. L. Dobretsov (1994), Geodynamic evolution of southern Siberia in Late Precambrian–Early Paleozoic time, in *Reconstruction of the Paleo-Asian Ocean*, edited by R. G. Coleman, pp. 45–62, VSP Int. Sci., Leiden, Netherlands.
- Berzin, N. A., R. G. Coleman, N. L. Dobretsov, L. O. Zonenshain, X. C. Xiao, and E. Chang (1994), Geodynamic map of the western part of the Paleo-Asian Ocean, *Russ. Geol. Geophys.*, *35*(7–8), 8–28.
- Besse, J., V. Courtillot, J. P. Pozzi, M. Westphal, and Y. X. Zhou (1984), Paleomagnetic estimates of crustal shortening in the Himalayan thrust and Zhangbo suture, *Nature*, *311*, 621–626, doi:10.1038/311621a0.
- Bibikova, E. V., et al. (1990), U-Pb, Sm-Nd and K-Ar ages of metamorphic and magmatic rocks of Pri-Olkhonye (western Pribaikaliye) (in Russian), in *Geology and Geochronology of the Precambrian Siberian Platform and Surrounding Fold Belts*, pp. 170–183, Nauka, St. Petersburg, Russia.
- Bukharov, A. A., V. A. Khalilov, T. M. Strakhova, and V. V. Chernikov (1992), The Baikal-Patom highland geology from the U-Pb dating of accessory zircon, *Geol. Geofiz.*, *12*, 29–39.
- Chen, A. (1998), Geometric and kinematic evolution of basement-cored structures: Intraplate orogenesis within the Yanshan orogen, northern China, *Tectonophysics*, *292*, 17–42, doi:10.1016/S0040-1951(98)00062-6.
- Chen, Y., and W. Chen (1997), *Mesozoic Volcanic Rocks: Chronology, Geochemistry and Tectonic Background*, 279 pp., Seismol. Press, Beijing.
- Cobbold, P. R., and P. Davy (1988), Indentation tectonics in nature and experiments, 2, central Asia, *Bull. Geol. Inst. Univ. Uppsala*, *14*, 143–162.
- Cocks, L. R. M., and T. H. Torsvik (2007), Siberia, the wandering northern terrane, and its changing geography through the Palaeozoic, *Earth Sci. Rev.*, *82*, 29–74, doi:10.1016/j.earscirev.2007.02.001.
- Darby, B. J., G. A. Davis, and Y. Zheng (2001a), Structural evolution of the southwestern Daqing Shan, Yinshan belt, Inner Mongolia, China, in *Paleozoic and Mesozoic Tectonic Evolution of Central Asia: From Continental Assembly to Intracontinental Deformation*, edited by M. S. Hendrix and G. A. Davis, *Mem. Geol. Soc. Am.*, *194*, 199–214.
- Darby, B. J., G. A. Davis, Y. Zheng, J. Zhang, and X. Wang (2001b), Evolving geometry of the Huhhot metamorphic core complex, Inner Mongolia, China, *Geol. Soc. Am. Abstr. Programs*, *32*, 33.
- Davis, G. A., X. Qian, Y. Zheng, H. M. Tong, C. Wang, G. E. Gehrels, M. Shafiqullah, and J. E. Fryxell (1996), Mesozoic deformation and plutonism in the Yunneng Shan: A metamorphic core complex north of Beijing, China, in *The Tectonic Evolution of Asia*, edited by A. Yin and T. M. Harrison, pp. 253–280, Cambridge Univ. Press, Cambridge, U. K.
- Davis, G. A., Y. Zheng, C. Wang, B. J. Darby, C. Zhang, and G. Gehrels (2001), Mesozoic tectonic evolution of the Yanshan fold and thrust belt, with emphasis on Hebei and Liaoning provinces, northern China, in *Paleozoic and Mesozoic Tectonic Evolution of Central Asia: From Continental Assembly to Intracontinental Deformation*, edited by M. S. Hendrix and G. A. Davis, *Mem. Geol. Soc. Am.*, *194*, 71–97.
- Davis, G. A., B. J. Darby, Y. Zheng, and T. L. Spell (2002), Geometric and temporal evolution of an extensional detachment fault, Hohhot metamorphic core complex, Inner Mongolia, China, *Geology*, *30*, 1003–1006, doi:10.1130/0091-7613(2002)030<1003:GATEOA>2.0.CO;2.
- Davy, P., and P. R. Cobbold (1988), Indentation tectonics in nature and experiments. Experiments scaled for gravity, *Bull. Geol. Inst. Uppsala*, *14*, 129–141.
- de Boissroglier, T., C. Petit, M. Fournier, P. Leturny, J.-C. Ringenbach, V. A. San'kov, S. A. Anisimova, and S. N. Kovalenko (2009), Palaeozoic orogenesis around the Siberian craton: Structure and evolution of the Patom belt and foredeep, *Tectonics*, *28*, TC1005, doi:10.1029/2007TC002210.
- De Grave, J., and P. Van den haute (2002), Denudation and cooling of the Lake Teletskoye region in the Altai Mountains (south Siberia) as revealed by apatite fission-track thermochronology, *Tectonophysics*, *349*, 145–159, doi:10.1016/S0040-1951(02)00051-3.
- Delvaux, D. (1997), Geodynamics of the Baikal rifting: New developments and perspectives, in *Lithospheric Structure, Evolution and Sedimentation in Continental Rifts*, edited by A. W. B. Jacobs, D. Delvaux, and M. A. Khan, *Commun. Dublin Inst. Adv. Stud., Ser. D. Geophys. Bull.*, *48*, 86–97.
- Delvaux, D., R. Moeys, G. Stapel, A. Melnikov, and V. Ermikov (1995a), Palaeostress reconstructions and geodynamics of the Baikal region, central Asia, Part I. Palaeozoic and Mesozoic pre-rift evolution, *Tectonophysics*, *252*, 61–101, doi:10.1016/0040-1951(95)00090-9.
- Delvaux, D., K. Theunissen, R. Van der Meer, and N. A. Berzin (1995b), Dynamics and paleostress of the Cenozoic Kurai-Chuya depression of Gornii Altai (south Siberia): Tectonic and climatic control, *Russ. Geol. Geophys.*, *36*(10), 26–45.
- Delvaux, D., R. Moeys, G. Stapel, C. Petit, K. Levi, A. Miroschnichenko, V. Ruzhich, and V. San'kov (1997), Paleostress reconstructions and geodynamics of the Baikal region, central Asia, Part 2. Cenozoic rifting, *Tectonophysics*, *282*, 1–38, doi:10.1016/S0040-1951(97)00210-2.
- Dobretsov, N. L., E. G. Konnikov, and N. N. Dobretsov (1992), Precambrian ophiolite belts of southern Siberia, Russia and their metallogeny, *Precambrian Res.*, *58*, 427–446, doi:10.1016/0301-9268(92)90128-B.
- Dunkl, I. (2002), TRACKKEY: A Windows program for calculation and graphical presentation of fission track data, *Comput. Geosci.*, *28*(1), 3–12, doi:10.1016/S0098-3004(01)00024-3.
- Enkin, R., Z. Yang, Y. Chen, and V. Courtillot (1992), Paleomagnetic constraints on the geodynamic history of the major blocks of China from the Permian to the Present, *J. Geophys. Res.*, *97*, 13,953–13,989, doi:10.1029/92JB00648.
- Epov, M. I., N. N. Nevedrova, and A. M. Sanchaa (2007), A geoelectrical model of the Barguzin basin in the Baikal Rift Zone, *Russ. Geol. Geophys.*, *48*, 626–641, doi:10.1016/j.rgg.2007.06.001.
- Ermikov, V. D. (1994), Mesozoic precursors of rift structures of central Asia, *Bull. Cent. Rech. Explor. Prod. Elf Aquitaine*, *18*(1), 123–134.
- Fan, W. M., F. Guo, Y. J. Wang, and G. Lin (2003), Late Mesozoic calc-alkaline volcanism of post-orogenic extension in the northern Da Hinggan Mountains, northeastern China, *J. Volcanol. Geotherm. Res.*, *121*, 115–135, doi:10.1016/S0377-0273(02)00415-8.
- Fedorovskii, V. S., L. F. Dobrzhimetskaya, T. V. Molchanova, and A. B. Likhachev (1993), New type of melange: The Baikal Lake, Ol'khon region, *Geotektonika*, *4*, 30–45.
- Filippova, I. B. (1969), The Khangay synclinorium: Main features of structure and evolution (in Russian), *Geotektonika*, *5*, 76–78.
- Florensov, N. A. (1960), *Mesozoic and Cenozoic Basins in the Baikal Region* (in Russian), Izd. Akad. Nauk SSSR, Moscow.
- Florensov, N. A., (Ed.) (1982), *The Pliocene and Pleistocene Stratigraphy of the Central Baikal Basin* (in Russian), Nauka, Novosibirsk, Russia.
- Fournier, M., L. Jolivet, P. Huchon, V. S. Rozhdvestvensky, K. F. Sergeev, and L. Osorbin (1994), Neogene strike-slip faulting in Sakhalin, and the Japan Sea opening, *J. Geophys. Res.*, *99*, 2701–2725, doi:10.1029/93JB02026.
- Fournier, M., L. Jolivet, P. Davy, and J. C. Thomas (2004), Back arc extension and collision: An experimental approach of the tectonics of Asia, *Geophys. J. Int.*, *157*, 871–889, doi:10.1111/j.1365-246X.2004.02223.x.
- Gao, S. S., K. H. Liu, P. M. Davis, P. D. Slack, Y. A. Zorin, V. V. Mordvinova, and V. M. Kozhevnikov

- (2003), Evidence for small-scale mantle convection in the upper mantle beneath the Baikal rift zone, *J. Geophys. Res.*, *108*(B4), 2194, doi:10.1029/2002JB002039.
- Gibsher, A. S., A. E. Izokh, and E. V. Khain (1993), Geodynamic evolution of northern segment of the Paleo-Asian ocean in Late Riphean–Early Paleozoic, in *Proceedings of the 4th International Symposium of IGC Project 283: Geodynamic Evolution of the Paleo-Asian Ocean, Novosibirsk, 15–24 June*, edited by N. L. Dobretsov and N. A. Berzin, pp. 67–69, Nauka, Novosibirsk, Russia.
- Graham, S. A., M. S. Hendrix, C. L. Johnson, D. Badamgarav, G. Badarch, J. Amory, M. Porte, R. Barsbold, L. E. Webb, and B. R. Hacker (2001), Sedimentary record and tectonic implications of Mesozoic rifting in southern Mongolia, *Geol. Soc. Am. Bull.*, *113*, 1560–1579, doi:10.1130/0016-7606(2001)113<1560:SRATIO>2.0.CO;2.
- Gusev, G. S., and V. Y. Khain (1996), On relations between the Baikal-Vitim, Aldan Stanovoy, and Mongol-Okhotsk terranes (south of mid-Siberia), *Geotectonics, Engl. Transl.*, *29*(5), 422–436.
- Hurford, A. J. (1990), Standardization of fission track dating calibration: Recommendation by the Fission track Working Group of the I.U.G.S. Subcommittee on Geochronology, *Chem. Geol.*, *80*, 171–178, doi:10.1016/0168-9622(90)90025-8.
- Hurford, A. J., and P. F. Green (1983), The zeta age calibration of fission-track dating, *Chem. Geol.*, *1*, 285–317.
- Hutchinson, D. R., A. J. Golmshtok, L. P. Zonenshain, T. C. Moore, C. A. Scholtz, and K. D. Klitgord (1992), Depositional and tectonic framework of the rift basins of Lake Baikal from multichannel seismic data, *Geology*, *20*, 589–592, doi:10.1130/0091-7613(1992)020<0589:DATFOT>2.3.CO;2.
- Ivanov, A. V. (2004), One rift, two models, *Sci. First Hand*, *1*, 50–62.
- Jin, J., Q. R. Meng, Y. Zhang, and D. Xu (2000), Jurassic-Cretaceous evolution of the Yingen basin and its petroleum potential, *Acta Petrol. Sin.*, *21*, 13–19.
- Johnson, J. S., S. A. Gibson, R. N. Thompson, and G. M. Nowell (2005), Volcanism in the Vitim Volcanic Field, Siberia: Geochemical evidence for a mantle plume beneath the Baikal rift zone, *J. Petrol.*, *46*, 1309–1344, doi:10.1093/ptrology/egi016.
- Jolivet, L., P. Davy, and P. Cobbold (1990), Right-lateral shear along the northwest Pacific margin and the India-Eurasia collision, *Tectonics*, *9*, 1409–1419, doi:10.1029/TC009i06p01409.
- Jolivet, L., M. Fournier, P. Huchon, V. S. Rozhdvenstskiy, S. Sergeyev, and L. S. Osorbin (1992), Cenozoic intracontinental dextral motion in the Okhotsk-Japan Sea region, *Tectonics*, *11*, 968–977, doi:10.1029/92TC00337.
- Jolivet, M., et al. (2007), The Mongolian summits: An uplifted, flat, old but still preserved erosion surface, *Geology*, *35*, 871–874, doi:10.1130/G23758A.1.
- Kashik, S. A., and V. N. Masilov (1994), Main stages and paleogeography of Cenozoic sedimentation in the Baikal rift system (eastern Siberia), *Bull. Cent. Rech. Explor. Prod. Elf Aquitaine*, *18*, 453–461.
- Kazansky, A. Y., D. V. Metelkin, V. Y. Bragin, and L. V. Kungurtsev (2005), Paleomagnetism of the Permian-Triassic traps from the Kuznetsk Basin, southern Siberia, *Russian Geol. Geophys.*, *46*(11), 1089–1102.
- Ketcham, R. A., R. A. Donelick, and M. B. Donelick (2000), AFTSolve: A program for multikinetic modelling of apatite fission-track data, *Geol. Mater. Res.*, *2*, 1–32.
- Khain, V. Y., and N. A. Bozhko (1988), *Historical Geotectonics: Precambrian*, 382 pp., Nedra, Moscow.
- Kimura, G., and K. Tamaki (1986), Collision, rotation and back arc spreading: The case of the Okhotsk and Japan seas, *Tectonics*, *5*, 389–401.
- Kimura, G., T. Tasaki, and M. Kono (1990), Mesozoic collision-extrusion tectonics in eastern Asia, *Tectonophysics*, *181*, 15–23, doi:10.1016/0040-1951(90)90005-S.
- Kiselev, A. I., H. A. Golovko, and M. E. Medvedev (1978), Petrochemistry of Cenozoic basalts and associated rocks in the Baikal rift zone, *Tectonophysics*, *45*, 49–59, doi:10.1016/0040-1951(78)90223-8.
- Kravchinsky, V. A., J.-P. Cogné, W. P. Harbert, and M. I. Kuzmin (2002), Evolution of the Mongol-Okhotsk Ocean as constrained by new palaeomagnetic data from the Mongol-Okhotsk suture zone, Siberia, *Geophys. J. Int.*, *148*, 34–57, doi:10.1046/j.1365-246x.2002.01557.x.
- Kulakov, I. Y. (2008), Upper mantle structure beneath southern Siberia and Mongolia, from regional seismic tomography, *Russ. Geol. Geophys.*, *49*, 187–196.
- Kuzmin, M. I., E. B. Karabanov, A. A. Prokopenko, V. F. Gelety, V. S. Antipin, D. F. Williams, and A. N. Gvozdkov (2000), Sedimentation processes and new age constraints on rifting stages in Lake Baikal: Results of deep-water drilling, *Int. J. Earth Sci.*, *89*, 183–192.
- Larroque, C., J.-F. Ritz, J.-F. Stephan, V. Sankov, A. Arjannikova, E. Calais, J. Deverchère, and L. Loncke (2001), Interaction compression-extension à la limite Mongolie-Sibérie: Analyse préliminaire des déformations récentes et actuelles dans le bassin de Tunka, *C.R. Acad. Sci.*, *332*, 177–184.
- Laslett, G. M., P. F. Green, I. R. Duddy, and A. J. W. Gleadow (1987), Thermal annealing of fission tracks in apatite. 2. A quantitative analysis, *Chem. Geol.*, *65*, 1–13, doi:10.1016/0009-2541(87)90189-6.
- Lebedev, S., T. Meier, and R. D. Van der Hilst (2006), Asthenospheric flow and origin of volcanism in the Baikal rift area, *Earth Planet. Sci. Lett.*, *249*, 415–424, doi:10.1016/j.epsl.2006.07.007.
- Lesne, O., E. Calais, and J. Déverchère (1998), Finite element modeling of present-day kinematics and strain in the Baikal rift zone, Siberia, *Tectonophysics*, *289*, 327–340, doi:10.1016/S0040-1951(98)00004-3.
- Levi, K., A. I. Miroshnichenko, V. A. San'kov, S. M. Babushkin, G. V. Larkin, A. A. Badardinov, H. K. Wong, S. Colman, and D. Delvaux (1997), Active faults of the Baikal Depression, *Bull. Cent. Rech. Explor. Prod. Elf Aquitaine*, *21*, 399–434.
- Lin, W., M. Faure, S. Nomade, Q. Shang, and P. R. Renne (2008), Permian-Triassic amalgamation of Asia: Evidence from northeast China sutures and their place in the final collision of north China and Siberia, *C. R. Geosci.*, *340*, 190–201, doi:10.1016/j.crte.2007.10.008.
- Logatchev, N. (1993), History and geodynamics of the Baikal rift in the context of Eastern Siberia rift system: A review, *Bull. Cent. Rech. Explor. Prod. Elf Aquitaine*, *17*(2), 353–370.
- Logatchev, N. A. (2003), History and Geodynamics of the Baikal rift, *Geol. Geofiz.*, *44*(5), 391–406.
- Logatchev, N. A., and Y. A. Zorin (1987), Evidence and causes for the two-stage development of the Baikal rift, *Tectonophysics*, *143*, 225–234, doi:10.1016/0040-1951(87)90092-8.
- Logatchev, N. A., et al. (1996), Cenozoic Rifting in the Continental Lithosphere, in *The Lithosphere of Central Asia*, pp. 57–80, Nauka, Novosibirsk, Russia.
- Logatchev, N. A., et al. (2002), K-Ar dating of the Paleocene weathering crust in the Baikal region, *Dokl. Akad. Nauk*, *385*(6), 797–799.
- Lunina, O. V., and A. S. Gladkov (2007), Late Cenozoic fault pattern and stress fields in the Barguzin rift (Baikal region), *Russ. Geol. Geophys.*, *48*, 598–609, doi:10.1016/j.rgg.2006.06.001.
- Malitch, N. S. (Ed.) (1999), Geological map of the Siberian Platform and Adjoining Areas, scale 1:1,500,000, Minist. of Nat. Resour. of Russ. Fed., Moscow.
- Mats, V. D. (1985), New data on the stratigraphy of Miocene and Pliocene rocks in the southern Baikal region, in *Problems of Geology and Paleogeography of Siberia and the Russian Far East*, pp. 36–53, Irkutsk Geol. Univ., Irkutsk, Russia.
- Mats, V. D. (1993), The structure and development of the Baikal rift depression, *Earth Sci. Rev.*, *34*, 81–118, doi:10.1016/0012-8252(93)90028-6.
- Mats, V. D., O. M. Khlystov, M. De Batist, S. Ceramicola, T. K. Lomonosova, and A. Klimansky (2000), Evolution of the Adamician Ridge Accommodation Zone in the central part of the Baikal rift, from high-resolution reflection seismic profiling and geological field investigations, *Int. J. Earth Sci.*, *89*, 229–250, doi:10.1007/s005310000094.
- Mats, V. D., G. F. Ufimtsev, and M. M. Mandel'baum (2001), *Cenozoic of the Baikal Rift Depression: Structure and Geological History*, Sibirskoe Otdelenie Rossijskaâ Akad. Nauka Filial Geo, Novosibirsk, Russia.
- Melnikov, A. I., A. M. Mazukabzov, E. V. Sklyarov, and E. P. Vasiliev (1994), Baikal rift basement: Structure and tectonic evolution, *Bull. Cent. Rech. Explor. Prod. Elf Aquitaine*, *18*(1), 99–122.
- Meng, Q.-R. (2003), What drove late Mesozoic extension of the northern China-Mongolia tract?, *Tectonophysics*, *369*, 155–174, doi:10.1016/S0040-1951(03)00195-1.
- Metelkin, D. V., I. V. Gordienko, and X. Zhao (2004), Paleomagnetism of Early Cretaceous volcanic rocks from Transbaikalia: Argument for Mesozoic strike-slip motions in central Asian structure, *Russ. Geol. Geophys.*, *45*(12), 1404–1417.
- Metelkin, D. V., I. V. Gordienko, and V. S. Klimuk (2007), Paleomagnetism of Upper Jurassic basalts from Transbaikalia: New data on the time of closure of the Mongol-Okhotsk ocean and Mesozoic intraplate tectonics of central Asia, *Russ. Geol. Geophys.*, *48*, 825–834, doi:10.1016/j.rgg.2007.09.004.
- Molnar, P., and P. Tapponnier (1975), Cenozoic tectonics of Asia: Effects of a continental collision, *Science*, *189*, 419–426, doi:10.1126/science.189.4201.419.
- Moore, T. C., K. D. Klitgord, A. J. Golmshtok, and E. Weber (1997), Sedimentation and subsidence patterns in the central and north basins of Lake Baikal from seismic stratigraphy, *Geol. Soc. Am. Bull.*, *109*, 746–766, doi:10.1130/0016-7606(1997)109<0746:SASPT>2.3.CO;2.
- Mushnikov, A. F., K. K. Anashkina, and B. I. Oleksiv (1966), Stratigraphy of Jurassic sediments in the eastern Trans-Baikal region (in Russian), *Bull. Geol. Miner. Resour. Chita Reg.*, *2*, pp. 57–99, Nedra, Moscow.
- Nevedrova, N. N., and M. I. Epov (2003), Deep geoelectrical soundings in active seismic areas, in *Geodynamics and Geocological Problems of Mountain Regions, Proceedings of the International Symposium, Bishkek, 27 Oct. to 3 Nov.*, pp. 153–163, Bishkek, Kyrgyzstan.
- Nie, S., D. B. Rowley, and A. M. Ziegler (1990), Constraints on the location of Asian microcontinents in Paleo-Tethys during Late Palaeozoic, in *Palaeozoic Palaeogeography and Biogeography*, edited by W. S. McKerrow and C. R. Scotese, *Mem. Geol. Soc.*, *12*, 397–409.
- Nikohyev, V. G., L. A. Vanyakin, V. V. Kalinin, and V. Y. Milanovskiy (1985), The sedimentary section beneath Lake Baikal, *Int. Geol. Rev.*, *27*, 449–459, doi:10.1080/00206818509466432.
- O'Sullivan, P. B., and R. R. Parrish (1995), The importance of apatite composition and single-grain ages when interpreting fission track data from plutonic rocks: A case study from the Coast Ranges, British Columbia, *Earth Planet. Sci. Lett.*, *132*, 213–224, doi:10.1016/0012-821X(95)00058-K.
- Patriat, P., and J. A. Chacón (1984), India-Eurasia collision chronology has implications for crustal shortening and driving mechanism of plates, *Nature*, *311*(5987), 615–621, doi:10.1038/311615a0.
- Patzelt, A., L. Huamei, W. Junda, and E. Appel (1996), Paleomagnetism of Cretaceous to tertiary sediments from southern Tibet: Evidence for the extent

- of the northern margin of India prior to the collision with Eurasia, *Tectonophysics*, 259, 259–284, doi:10.1016/0040-1951(95)00181-6.
- Petit, C., and J. Déverchère (2006), Structure and evolution of the Baikal rift: A synthesis, *Geochem. Geophys. Geosyst.*, 7, Q11016, doi:10.1029/2006GC001265.
- Petit, C., J. Déverchère, F. Houdry, V. A. San'kov, V. I. Melnikova, and D. Delvaux (1996), Present-day stress field changes along the Baikal rift and tectonic implications, *Tectonics*, 15, 1171–1191, doi:10.1029/96TC00624.
- Petit, C., J. Déverchère, E. Calais, V. A. San'kov, and D. Fairhead (2002), Deep structure and mechanical behavior of the lithosphere in the Hangai-Hövsögöl region, Mongolia: New constraints from gravity modelling, *Earth Planet. Sci. Lett.*, 197, 133–149, doi:10.1016/S0012-821X(02)00470-3.
- Petit, C., E. Burov, and C. Tiberi (2008), Strength of the lithosphere and strain localisation in the Baikal rift, *Earth Planet. Sci. Lett.*, 269, 523–529, doi:10.1016/j.epsl.2008.03.012.
- Prokopyev, A. V., J. Toro, E. L. Miller, and G. E. Gehrels (2008), The paleo-Lena River—200 m.y. of transcontinental zircon transport in Siberia, *Geology*, 36(9), 699–702, doi:10.1130/G24924A.1.
- Rassakov, S. V. (1993), *Magmatism of the Baikal Rift System* (in Russian), 141 pp., Nauka, Novosibirsk, Russia.
- Ren, J., K. Tamaki, S. Li, and Z. Junxia (2002), Late Mesozoic and Cenozoic rifting and its dynamic setting in eastern China and adjacent areas, *Tectonophysics*, 344, 175–205, doi:10.1016/S0040-1951(01)00271-2.
- Rezanov, I. N. (2000), Formation History of Paleogene Sediments in the Eravna Depression and its Mountainous Framing, in *Issues of Lithology, Geochemistry, and Metallogeny of Sedimentary Processes* (in Russian), pp. 158–163, GEOS 2, Moscow.
- Rutshtein, I. G. (Ed.) (1992), Geological map of the Chita Region, Chita, scale 1:500,000, 23 sheets, MPGIT, Moscow.
- Sarkisyan, S. G. (1958), *Mesozoic and Tertiary Sediments of the Baikal and Trans-Baikal Regions and the Russian Far East* (in Russian), Izd. Akad. Nauk SSSR, Moscow.
- Scholz, C. A., and D. R. Hutchinson (2000), Stratigraphic and structural evolution of the Selenga Delta Accommodation Zone, Lake Baikal rift, Siberia, *Int. J. Earth Sci.*, 89, 212–228, doi:10.1007/s005310000095.
- Sengör, A. M. C., and K. Burke (1978), Relative timing of rifting and volcanism on Earth and its tectonic implications, *Geophys. Res. Lett.*, 5, 419–421, doi:10.1029/GL005i006p00419.
- Shao, J., B. Mu, and L. Zhang (2000), Deep geological process and its shallow response during Mesozoic transfer of tectonic framework in eastern north China, *Geol. Rev.*, 46, 32–40.
- Shao, J., X. Li, and L. Zhang (2001), The geochemical condition for genetic mechanism of the Mesozoic bimodal dyke swarms in Nankou-Jiugongguan (in Chinese with English abstract), *Geochimica*, 30, 517–524.
- Skoblo, V. M., N. A. Lyamina, and I. V. Luzina (2001), *The Continental Upper Mesozoic of the Baikal and Transbaikalian Regions* (in Russian), Sibirskoe Otdelenie Rossijskaja Akad. Nauka, Novosibirsk, Russia.
- Solonenko, V. P. (1968), *Seismotectonics and Seismicity of the Baikal Rift System* (in Russian), Nauka, Moscow.
- Solonenko, V. P. (1981), *Seismogeology and Detailed Seismic Zoning of the Baikal Region* (in Russian), Nauka, Novosibirsk, Russia.
- Song, J., and L. Dou (1997), *Mesozoic-Cenozoic Tectonics of Petroleum Basins in eastern China and Their Petroleum Systems*, 182 pp., Pet. Ind. Press, Beijing.
- Spicer, R. A., A. Ahlberg, A. B. Herman, C.-C. Hofmann, M. Raikovich, P. J. Valdes, and P. J. Markwick (2008), The Late Cretaceous continental interior of Siberia: A challenge for climate models, *Earth Planet. Sci. Lett.*, 267, 228–235, doi:10.1016/j.epsl.2007.11.049.
- Srytevsev, N. A., V. A. Khalilov, V. V. Buldygerov, and V. I. Perelyaev (1992), Geochronology of the Baikal-Muya belt granitoid, *Geol. Geofiz.*, 9, 72–77.
- Suvorov, V. D., Z. M. Mishenkina, G. V. Petrick, I. F. Sheludko, V. S. Seleznev, and V. M. Solovoyov (2002), Structure of the crust in the Baikal Rift Zone and adjacent areas from deep seismic sounding data, *Tectonophysics*, 351, 61–74, doi:10.1016/S0040-1951(02)00125-7.
- Tapponnier, P., and P. Molnar (1979), Active faulting and Cenozoic tectonics of the Tien Shan, Mongolia and Baykal regions, *J. Geophys. Res.*, 84, 3425–3455, doi:10.1029/JB084iB07p03425.
- Tauson, L. V., V. S. Antipin, M. N. Zakharov, and V. S. Zubkov (1984), *Geochemistry of Mesozoic Latites of the Trans-Baikal Region* (in Russian), 213 pp., Nauka, Novosibirsk, Russia.
- ten Brink, U. S., and M. H. Taylor (2002), Crustal structure of central Lake Baikal: Insights into intracontinental rifting, *J. Geophys. Res.*, 107(B7), 2132, doi:10.1029/2001JB000300.
- Tiberi, C., M. Diamant, J. Déverchère, C. Petit-Mariani, V. Mikhailov, S. Tikhotsky, and U. Achauer (2003), Deep structure of the Baikal rift zone revealed by joint inversion of gravity and seismology, *J. Geophys. Res.*, 108(B3), 2133, doi:10.1029/2002JB001880.
- Traynor, J. J., and C. Sladen (1995), Tectonic and stratigraphic evolution of the Mongolian People's Republic and its influence on hydrocarbon geology and potential, *Mar. Pet. Geol.*, 12, 35–52, doi:10.1016/0264-8172(95)90386-X.
- Tsekhovskiy, Y. G., and M. G. Leonov (2007), Sedimentary formations and main development stages of the western Transbaikalian and southeastern Baikal regions in the Late Cretaceous and Cenozoic, *Lithol. Miner. Resour.*, 42(4), 349–362, doi:10.1134/S0024490207040037.
- van der Beek, P., D. Delvaux, P. A. M. Andriessen, and K. G. Levi (1996), Early Cretaceous denudation related to convergent tectonics in the Baikal region, SE Siberia, *J. Geol. Soc.*, 153, 515–523, doi:10.1144/gsjgs.153.4.0515.
- Vassallo, R., M. Jolivet, J.-F. Ritz, R. Braucher, C. Larroque, C. Sue, M. Todbileg, and D. Javkhlanbold (2007), Uplift age and rates of the Gurvan Bogd system (Gobi-Altay) by apatite fission track analysis, *Earth Planet. Sci. Lett.*, 259, doi:10.1016/j.epsl.2007.04.047.
- Wang, F., X. H. Zhou, L. C. Zhang, J. F. Ying, Y. T. Zhang, F. Y. Wu, and R. X. Zhu (2006), Late Mesozoic volcanism in the Great Xing'an Range (NE China): Timing and implications for the dynamic setting of NE Asia, *Earth Planet. Sci. Lett.*, 251, 179–198, doi:10.1016/j.epsl.2006.09.007.
- Watson, M. P., A. B. Hayward, D. N. Parkinson, and Z. M. Zhang (1987), Plate tectonic history, basin development and petroleum source rock deposition onshore China, *Mar. Pet. Geol.*, 4, 205–225, doi:10.1016/0264-8172(87)90045-6.
- Webb, L. E., S. A. Graham, C. L. Johnson, G. Badarch, and M. S. Hendrix (1999), Occurrence, age and implications of the Yagan-Onch Hayrhan metamorphic core complex, southern Mongolia, *Geology*, 27(2), 143–146, doi:10.1130/0091-7613(1999)027<0143:OAAIOT>2.3.CO;2.
- Windley, B. F., and M. B. Allen (1993), Mongolia plateau: Evidence for a late Cenozoic mantle plume beneath central Asia, *Geology*, 21, 295–298, doi:10.1130/0091-7613(1993)021<0295:MPEFAL>2.3.CO;2.
- Worrall, D. M., V. Kruglyak, F. Kunst, and V. Kusnetsov (1996), Tertiary tectonics of the Sea of Okhotsk, Russia: Far-field effects of the India-Asia collision, *Tectonics*, 15, 813–826, doi:10.1029/95TC03684.
- Yang, G., Y. Chai, and Z. Wu (2001), Thin-skinned thrust structures in western Liaoning in eastern sector of the Yanshan orogenic belt, *Dizhi Xuebao*, 75, 321–332.
- Yarmolyuk, V. V., and V. G. Ivanov (2000), Late Mesozoic and Cenozoic magmatism and geodynamics of western Transbaikalia, *Geotektonika*, 34(2), 43–64.
- Yarmolyuk, V. V., and V. I. Kovalenko (2001), The Mesozoic-Cenozoic of Mongolia, in *Tectonics, Magmatism, and Metallogeny of Mongolia*, edited by A. B. Dergunov, pp. 203–244, Taylor and Francis, London.
- Yarmolyuk, V. V., V. I. Kovalenko, A. B. Kotov, and E. B. Salmikova (1997), The Angara-Vitim batholith: Geodynamics of batholith formation in the Central Asian fold belt (in Russian), *Geotektonika*, 5, 18–32.
- Zhao, X., R. S. Coe, Y. Zhou, H. Wu, and J. Wang (1990), New paleomagnetic results from northern China: Collision and suturing with Siberia and Kazakhstan, *Tectonophysics*, 181, 43–81, doi:10.1016/0040-1951(90)90008-V.
- Zheng, Y., S. Wang, and Y. Wang (1991), An enormous thrust nappe and extensional metamorphic core complex in Sino-Mongolian boundary area, *Sci. China*, 34, 1145–1152.
- Zheng, Y., Q. Zhang, Y. Wang, R. Liu, S. G. Wang, G. Zuo, S. Z. Wang, B. Lkaasuren, G. Badarch, and Z. Badamgarav (1996), Great Jurassic thrust sheets in Beishan (North Mountains): Gobi area of China and Southern Mongolia, *J. Struct. Geol.*, 18, 1111–1126, doi:10.1016/0191-8141(96)00038-7.
- Zheng, Y., G. A. Davis, C. Wang, B. J. Darby, and Y. Hua (1998), Major thrust system in the Daqing Shan, Inner Mongolia, China, *Sci. China*, 41(5), 553–560.
- Zonenshain, L. P., and L. A. Savostin (1981), Geodynamics of the Baikal rift zone and plate tectonics of Asia, *Tectonophysics*, 76, 1–45, doi:10.1016/0040-1951(81)90251-1.
- Zonenshain, L. P., M. I. Kuzmin, and L. M. Natapov (1990a), *The URSS Territory Plate Tectonics*, vol. 1, 328 pp., Nedra, Moscow.
- Zonenshain, L. P., M. I. Kuzmin, and L. M. Natapov (1990b), *The URSS Territory Plate Tectonics*, vol. 2, 334 pp., Nedra, Moscow.
- Zorin, Y. A. (1981), The Baikal rift: An example of intrusion of asthenospheric material into the lithosphere as the cause of disruption of lithospheric plates, *Tectonophysics*, 73, 91–104, doi:10.1016/0040-1951(81)90176-1.
- Zorin, Y. A. (1999), Geodynamics of the western part of the Mongolia-Okhotsk collisional belt, Trans-Baikalian region (Russia) and Mongolia, *Tectonophysics*, 306, 33–56, doi:10.1016/S0040-1951(99)00042-6.
- Zorin, Y. A., M. R. Novoselova, E. K. Turutanov, and V. M. Kozhevnikov (1990), Structure of the lithosphere in the Mongolia-Siberian mountainous province, *J. Geodyn.*, 11, 327–342, doi:10.1016/0264-3707(90)90015-M.
- Zorin, Y. A., et al. (1993), The south Siberia—central Mongolia transect, *Tectonophysics*, 225, 361–378, doi:10.1016/0040-1951(93)90305-4.
- Zorin, Y. A., V. G. Belichenko, E. K. Turutanov, V. V. Mordvinova, P. Khosbayar, O. Tomurtogov, N. Arvisbaatar, S. Gao, and P. Davis (1994), The Baikal-Mongolia transect (in Russian), *Russ. Geol. Geophys.*, 7–8, 94–110.
- Zorin, Y. A., V. V. Mordvinova, E. K. Turutanov, B. G. Belichenko, A. A. Artemyev, G. L. Kosarev, and S. S. Gao (2002), Low seismic velocity layers in the Earth's crust beneath eastern Siberia (Russia) and central Mongolia: Receiver function data and their possible geological implication, *Tectonophysics*, 359, 307–327, doi:10.1016/S0040-1951(02)00531-0.

Zorin, Y. A., E. K. Turutanov, V. V. Mordvinova, V. M. Kozhevnikov, T. B. Yanovskaya, and A. V. Treusov (2003), The Baikal rift zone: The effect of mantle plumes on older structure, *Tectonophysics*, 371, 153–173, doi:10.1016/S0040-1951(03)00214-2.

Earth Crust, 128 Lermontova Avenue, 664033 Irkutsk, Russia.

T. De Boisgrollier, M. Fournier, and C. Petit, Laboratoire de Tectonique, UMR 7072, Université Pierre et Marie Curie–Paris 6, CNRS, 4, Place Jussieu, F-75252 Paris, France.

M. Jolivet, Laboratoire Géosciences Montpellier, UMR 5243, Université Montpellier II, CNRS, F-34095 Montpellier, France. (jolivet@gm.univ-montp2.fr)

J.-C. Ringenbach, Total, Tour Coupole, 2 place de la coupole, F-92400 Courbevoie CEDEX, France.

---

S. V. Anisimova, L. Byzov, S. N. Kovalenko, A. I. Miroshnichenko, and V. A. Sankov, Institute of the